High Level Examination of Am-241 as an Alternative Fuel Source in Radioisotope Thermoelectric Generators

A Thesis

Presented in Partial Fulfilment of the Requirements for the

Degree of Master of Science

with a

Major in Nuclear Engineering

in the

College of Graduate Studies

University of Idaho

by

Jeremiah S. Dustin

Major Professor: R. A. Borrelli, Ph.D.

Committee Members: Michael Haney, Ph.D.; J. Stephen Herring, Ph.D.

Department Administrator: Richard Christensen, Ph.D.

August 2020

Authorization to Submit Thesis

This thesis of Jeremiah Seth Dustin, submitted for the degree of Master of Science with a major in Nuclear Engineering and titled "High Level Examination of Am-241 as an Alternative Fuel Source in Radioisotope Thermoelectric Generators," has been reviewed in final form. Permission, as indicated by the signatures and dates given below, is now granted to submit final copies to the College of Graduate Studies for approval.

Major Professor: _____Date_____
Robert Borrelli, Ph.D.

Committee Members: _____Date_____
Michael Haney, Ph.D.

_____Date_____
J. Stephen Herring, Ph.D.

Department Administrator: _____Date_____
Richard Christensen, Ph.D.

Abstract

Radioisotope thermoelectric generators (RTGs) have been utilized in the USA to power satellites and other space exploration equipment for over half a century. RTGs are essential for deep space exploration where solar energy is negligible. ^{238}Pu is the current fuel source for RTGs due to several favorable properties, such as high decay heat and minimal gamma radiation emission. The supply of ^{238}Pu is dwindling rapidly, but ^{241}Am has emerged as a potential substitute.

We have assessed the performance of ^{241}Am as an alternative to ^{238}Pu by modeling the specific decay-heat and gamma spectra of several potential radioisotopes in SCALE-ORIGEN, and comparing these with ^{238}Pu. An analysis of half-life, paired with decay heat and gamma output demonstrated that, of the isotopes reviewed, ^{241}Am had the greatest potential for replacing ^{238}Pu, with additional design considerations. ^{241}Am had a specific decay heat about 1/5th that of ^{238}Pu, and emits gamma radiation at about 50 keV. This leads to additional mass requirements for fuel and possibly shielding.

Due to the potential health effects for operators, fabricators, and others with the potential to be exposed to these lower energy gammas, as well as impacts on sensitive electronics, we assessed radiation transport for an ^{241}Am powered Multi-Mission Radioisotope Thermoelectric Generator. We have modeled the use of americium as a fuel source replacement for plutonium in current MMRTG designs. The assessment has been performed using MCNP6, in terms of gamma emissions that might interfere with sensitive equipment and consequently the potential for additional shielding needed to mitigate such interference. The radiation transport of the ^{241}Am fueled model is compared with that of a ^{238}Pu fueled model.

Acknowledgements

I would like to thank my advisor, Dr. Bob Borrelli for giving me the opportunity to do this work. I would also like to thank Michael Smith of ORNL for his invaluable input at the beginning of this project.

Table of Contents

List of Tables

List of Figures

Chapter 1

Introduction

Radioisotope thermoelectric generators (RTGs) have been utilized in the USA to power satellites and other space exploration equipment for over a half century [1]. RTGs have no moving parts and are considered highly reliable and ideal for unmanned spacecraft [2]. ^{238}Pu, an alpha emitting by-product of nuclear weapons production is currently the fuel source for RTGs due to favorable properties such as an 87.7 year half-life, a high specific decay heat of 0.56 W/g, and minimal gamma radiation emission. An RTG was recently used by New Horizons, which rendezvoused with Pluto in July 2015 [3]. The Voyager I and II spacecrafts, launched in 1977, are still operational. This is in part due to power provided by RTGs. RTGs are essential to deep space exploration where available solar energy is negligible. However, the supply of the fuel source, ^{238}Pu, is dwindling rapidly and may be depleted by the end of the decade [4].

At Oak Ridge National Lab, production of ^{238}Pu has begun again in the USA for the first time since the 1980s, but the capability is new, and had not achieved a production scale. By 2015, 77 lbs of ^{238}Pu was available for use by NASA, with only about half of the supply meeting specifications for power production [5].

^{241}Am, the same radioisotope used in many household smoke detectors, has emerged as a possible substitute to ^{238}Pu in RTGs. ^{241}Am is potentially less expensive than ^{238}Pu [6]. It can be obtained from civil plutonium stockpiles, as it is produced as a natural result of uranium fission in civilian nuclear power plants and subsequent ^{241}Pu decay. The specific decay heat of ^{241}Am is about 20% that of ^{238}Pu, at 0.115 W/g, and exhibits higher intensity gamma emission, but ^{241}Am decays with a 432 year half-life [7] giving it favorable properties in terms of a useful lifespan.

We are assessing the performance of an ^{241}Am powered Multi Mission Radioisotope

Thermoelectric Generator (MMRTG) for use in long-term satellites for deep space exploration. We are modeling the use of americium as a fuel source as a replacement for plutonium for an MMRTG design using the MCNP (Monte Carlo N-Particle) code. This is a widely used computational tool for a broad variety of nuclear physics, science, and engineering problems [8]. By modeling both ^{238}Pu and ^{241}Am fueled MMRTG, the code for the americium fueled MMRTG can be used to compare radiation transport behavior of ^{238}Pu and ^{241}Am for similar geometries. With these models future work can be focused on the modification and development of shielding for the MMRTG model, as well as novel fuel loading configurations necessary to achieve the thermal output that would make an ^{241}Am fueled RTG technically feasible.

1.1 Background

Exploration of the solar system is essential for a wide range of scientific advancements. A subsurface ocean has been discovered on Europa [9], and is now considered a strong candidate for life beyond Earth. Triton, Neptune's largest moon, is geologically active and could have a subsurface ocean [10]. Pluto exhibits a wide variety of geology yet to be studied, and both Pluto and Charon show a high degree of geologic complexity [11]. New Horizons has already ventured one billion miles beyond Pluto to the edge of the solar system, into the Kuiper belt to meet Kuiper Belt Object (KBO) 2014 MU69 [12]. Data collected from missions such as these can reveal how the solar system was formed, if there is any potential for life within our own solar system, potential material resources, and promote general technological advancement.

1.1.1 Relevant Space Missions

At great distances from the sun, the use of solar energy to power space missions is not feasible. ^{238}Pu has been used as a heat source in RTGs for a half century history of space exploration. These RTGs are based on the scientific principle of the Seebeck effect,

where the application of a temperature difference between semiconductors produces a voltage difference [13]. A direct current can be obtained with an electrical circuit. In September 2016, the European Space Agency landed the Rosetta satellite on the 67P/Churyumov−Gerasimenko comet [18]. However, the satellite relied on solar panels to produce power. It landed in the shadow of a cliff and could not collect any solar power. The satellite ceased transmission after about two days. This underscores the need for RTGs in diverse aspects of space exploration.

^{238}Pu has been produced from the irradiation of ^{237}Np, which is a by-product of ^{239}Pu production. ^{238}Pu decays with an 87.7 year half-life via alpha particle emissions at 5.60 MeV, and very weak gamma emissions. While ideal as a heat source for RTG's, the supply of ^{238}Pu is quickly dwindling. As of 2013, there were only 36 pounds of usable ^{238}Pu earmarked for NASA; the Mars Curiosity rover requires 11 pounds of this [4]. While ^{237}Np is also produced in conventional nuclear power reactors, quantities of ^{238}Pu necessary for space exploration are relatively small compared to needs [14]. Therefore, it is prudent to pursue an alternative fuel source so as to maintain capabilities for scientific explorations of the solar system.

1.1.2 Radioisotope Characteristics

^{241}Am is currently being considered as a fuel source for use in RTGs [15] [16] [6]. ^{241}Am can be obtained directly from the reprocessing of used nuclear reactor fuel. Prior to reprocessing, used fuel is cooled, typically for 5 to 10 years. During the life of the fuel ^{241}Am is produced as a result of ^{241}Pu decay. Through reprocessing, americium and other actinide elements are separated from uranium and plutonium. Obtaining ^{241}Am requires minimal additional processing in comparison to the purification and subsequent irradiation of ^{237}Np. This results in a lower cost for ^{241}Am than ^{238}Pu [6] [16]. In the UK, which currently reprocesses used nuclear fuel, more than 100 tons of plutonium is currently in storage. This is resulting in a continually increasing supply of ^{241}Am [17]. ^{241}Am decays by alpha particle emission at 5.49 MeV, slightly less than ^{238}Pu, resulting

in a specific power of 0.115 W/g with non-negligible gamma ray emission [7]. ^{241}Am decays with a 432 year half-life, potentially providing a significantly longer life cycle for ^{241}Am RTGs.

For other ^{241}Am RTG proposed designs, a power output in the 10 W - 50 W range is targeted [19]. This allows for modular and scalable designs for a variety of mission objectives. The current RTG model for NASA is the Multi-Mission Radioisotope Thermoelectric Generator (MMRTG), which operates with ^{238}Pu. This is powering the Curiosity rover on Mars.

1.2 Literature Review

1.2.1 History

The United States' Systems for Nuclear Auxiliary Power (SNAP) Program was one of the first endeavors for turning heat from radioactive decay into usable electricity. SNAP-1 was the first of the dynamic isotope power generators for this program, which used a heat engine, rather than thermoelectrics. It used a Cerium-144 source with the aim of generating 500 W for 60 days. This dynamic generator was quickly abandoned for efforts in thermoelectric generation with the SNAP-1A unit. This endeavor was cancelled in 1959. SNAP-3 was the continuation of this effort, and on Jan 16, 1959 the Po-210 fueled, 1.8 kg device demonstrated it was capable of 11.6 kW/hrs-electric over 280 days [20]. While SNAP-3 demonstrated the potential for a radioisotope-fueled thermoelectric generator, all subsequent RTG's used in space missions were fueled by ^{238}Pu in one form or another [21], see table 1.1 for various RTG's, specifications, and fuel forms used by NASA from 1961-2001.

In the review of potential isotopes for RTG power systems, developers looked at four main criteria. The first criterion was safety. A radioisotope must not subject people to excess radiation. They also must have a reliable power availability, operating with stability over a reasonable time-period without failure. For space systems, it was

Table 1.1: RTGs used in space missions from 1961 to 2001 [21].

RTG ID ($\#\,of\ RTGs$)	Spacecraft	Launch Date	Power $W_{electric}$	Fuel Type
SNAP-3B (1)	Transit 4A	29 Jun 61	2.7	^{238}Pu Metal
SNAP-3B (1)	Transit 4B	15 Nov 61	2.7	^{238}Pu Metal
SNAP-9A (1)	Transit 5BN-1	28 Sep 63	26.8	^{238}Pu Metal
SNAP-9A (1)	Transit 5BN-2	05 Dec 63	26.8	^{238}Pu Metal
SNAP-9A (1)	Transit 5BN-3	21 Apr 64	26.8	^{238}Pu Metal
SNAP-19B2 (2)	Nimbus-B-1	18 May 68	30	$^{238}PuO_2$-Mo
SNAP-19B3 (2)	Nimbus III	14 Apr 69	30	$^{238}PuO_2$-Mo
SNAP-27 (1)	Apollo 12	14 Nov 69	75	$^{238}PuO_2$ Microspheres
SNAP-27 (1)	Apollo 13	11 Apr 70	63.5	$^{238}PuO_2$ Microspheres
SNAP-27 (1)	Apollo 14	31 Jan 71	73	$^{238}PuO_2$ Microspheres
SNAP-27 (1)	Apollo 15	26 Jul 71	76	$^{238}PuO_2$ Microspheres
SNAP-19 (4)	Pioneer 10	02 Mar 72	41.2	$^{238}PuO_2$-Mo
SNAP-27 (1)	Apollo 16	16 Apr 72	72	$^{238}PuO_2$ Microspheres
Transit-RTG (1)	Triad-01-1X	02 Sep 72	36.8	$^{238}PuO_2$-Mo
SNAP-27 (1)	Apollo 17	07 Dec 72	77	$^{238}PuO_2$ Microspheres
SNAP-19 (4)	Pioneer 11	05 Apr 73	41.2	$^{238}PuO_2$-Mo
SNAP-19 (2)	Viking 1	20 Aug 75	42.5	$^{238}PuO_2$-Mo
SNAP-19 (2)	Viking 2	09 Sep 75	42.5	$^{238}PuO_2$-Mo
MHW-RTG (2)	Les 8	14 Mar 76	152	$^{238}PuO_2$ Pellet
MHW-RTG (2)	Les 9	14 Mar 76	152	$^{238}PuO_2$ Pellet
MHW-RTG (3)	Voyager 2	20 Aug 77	159	$^{238}PuO_2$ Pellet
MHW-RTG (3)	Voyager 1	05 Sep 77	156	$^{238}PuO_2$ Pellet
GPHS-RTG (2)	Galileo	18 Oct 89	285	$^{238}PuO_2$ Pellet
GPHS-RTG (1)	Ulysses	06 Oct 90	285	$^{238}PuO_2$ Pellet
GPHS-RTG (3)	Cassini	15 Oct 97	285	$^{238}PuO_2$ Pellet

important for an isotope to have a reasonable power to weight ratio, as excess mass requires extra resources for a successful launch. The last criteria was that an isotope have reasonable availability with affordable production [22].

Based on these criteria, the US Atomic Energy Commission had identified several practical radioisotopes by 1963. The potential isotopes identified included cobalt-60, strontium-90, cesium-137, promethium-147, thulium-170, polonium-210, plutonium-238, and curium-244 [23]. Half-lives of these isotopes ranged from 0.35 years (Tm-170) to 87.6 years (Pu-238), with initial power densities from 0.22 W/g (CsCl) to 45 W/g (RePo). NASA identified several additional potential isotopes, including cesium-134, and cerium-144 [24]. Ultimately, it was determined that Pu-238 was the most viable option as a fuel

source, and was subsequently used to power all RTG's used in US space missions.

In past reviews of isotope selections by the former USSR, it was determined that the most useful radioisotopes will have half-lives between 100 days and 100 years. Additionally, alpha emitters are preferable due to the high level of power generation per decay [25]. As stated previously it is important to consider the availability and means of production for a potential isotope. This broad definition of usefulness led to the review of additional suitable radioisotopes, including actinium-227, thorium-228, uranium-232, promethium-147, and iridium-192. The former Soviet Union utilized Po-210 on at least two RTG space missions in the 1960's. They did not continue to pursue RTGs in space, instead favoring U-235 fueled-reactor thermoelectric generation.

1.2.2 Space Nuclear

From 1961 to 2006, the US had flown 41 RTGs and 1 nuclear reactor to power 24 systems. The USSR had flown at least 35 reactors and 2 RTGs to power 37 space systems [26]. Nuclear power is an important and enduring component of space exploration, especially in missions to deep space where solar flux is incapable of powering photovoltaic power systems.

Potential strategies have been identified for the use of RTGs in space exploration, beyond the traditional uses in deep space exploration. NASA has reviewed strategies for the use of contemporary RTGs, and applying the power conversion technology from these systems to simple nuclear reactors. These efforts would serve as a foundation for nuclear power systems which could be used in future space exploration missions [27], in a strategy for technology development similar to that of the Russian Space Program.

A review of future space mission requirements demonstrates a mission needs gap in the realm of small electric generating units <10 W electric, and the potential for a 1 W_e device. This gap cannot be filled with current US radioisotope fuel arrays. European Space programs are already considering the potential of a Am-241 fueled RTG, due to the availability and cost efficiency of this radioisotope. Initial performance requirements

have been assessed, resulting in theoretical units generating 1-2 W electric with a specific power of 0.7 - 0.9 W_e/kg using Bismuth Telluride Thermoelectrics [28].

Additional research is being performed on small power output (milliwatt scale) RTG's. These are being reviewed for potential uses in space power. These devices may offer a greater than 15 year service time with high reliability [29].

Other research directions in nuclear space power relate to enhancing the efficiency of the MMRTG. NASA awarded the original contract for the MMRTG to Boeing-Rocketdyne and subcontractor Teledyne Energy Systems. The MMRTG uses Lead-Telluride/Tellurium-Antimony-Germanium-Silver thermocouples, producing 123 watts with eight GPHS modules [30]. NASA has been anticipating mission needs greater than the capabilities of the MMRTG. As such, it had developed the goal of significantly increasing power conversion efficiency to reduce fuel requirements. NASA also funded research in innovative power conversion technology, the development of 100 W-electric modules, as well as milli-watt and multi-watt power conversion systems [31].

The current MMRTG design is being enhanced by increasing efficiency with new TC materials. The MMRTG thermal efficiency is currently 6% - 7%. That is, the fraction of thermal energy produced by the RTG converted to electrical power. The original materials were PbTe/TAGS. By replacing these TC's with skutterudite materials, a potential 25% power increase could be achieved initially, with a nearly 50% power increase at the end of the MMRTG life (defined as 17 years from fueling) through lower degradation of skutterudite material vs. PbTe/TAGS [32].

1.2.3 Selection

As technologies and methods have progressed in the production of radioisotopes, numerous isotopes are in common use today that may have been impractical to produce in the past [33]. As nuclear material has aged, isotopes in the form of decay products have also increased in abundance. For instance, the quantity of Am-241 has increased with the decay of nuclear waste. This increasingly available isotope can be separated from

waste to a high purity [34], while past unavailability of Am-241 limited its usefulness.

Research has been performed to reassess the viability of certain radioisotopes for use in thermoelectric generation [15]. Am-241, Po-208, Po-210, and Sr-90 were analyzed for safety and usability in an alternative RTG design. Goals for the study included minimizing dose rate and mass. Potential shielding requirements were reviewed, along with encapsulation technology. It was determined that Am-241 would be a viable option for RTGs based on thermal performance, neutron dose rates, and favorable half-life . It appears that Am-241 will be a viable option for future RTG-supported space missions. Nevertheless, it is prudent to identify and analyze additional radioisotopes in terms of their heat availability, half-lives, and radiation safety.

1.3 Scope

The objective of this project is to determine the most viable radioisotope of those assessed, and through computational modeling to determine the feasibility of replacement for ^{238}Pu fuel in an RTG. This will be accomplished through a review of potential radioisotopes. These isotopes are assessed in terms of their specific decay heat over time, gamma spectra, and cost/availability. The specific decay heat over time, as well as gamma spectra are found using the ORIGEN portion of the SCALE code. After reviewing this material, the most viable radioisotope will be used as an input in a Monte Carlo N-Particle transport model of an MMRTG and the radiation transport behavior will be reviewed.

Monte Carlo methods do not solve explicit transport equations, but rather they simulate many individual particles and record the average behavior. These codes can handle complex geometries well, with accurate cross sections, but these can be slow, only providing statistical results. These are not always efficient for space problems. MCNP is capable of tracking electrons, photons, protons, neutrons, and select ions. MCNP has the capacity to handle versatile geometry, and comprehensive physics [39]. An often perceived disadvantage of MCNP is its relative difficulty to learn versus other Monte

Carlo codes, such as NOVICE, ITS, TRIM, and CREME. None of these were viable for the problem at hand, due to the complex geometry of the MMRTG and source selection required.

Past work has been performed to determine dose rates for RTGs fueled by Pu-238. Pu-238 has very low spontaneous fission and gamma emissions, but low concentrations of Pu-236 exist as impurities in RTG fuel. These isotopes spontaneously fission and produce neutrons. A decay product of Pu-236 is Tl-208, which generates 2.6 MeV gamma rays [35]. This demonstrates the need for tracking dose from the fuel source of an RTG, even if that fuel is nominally safe.

1.3.1 Goals

This work is not specifically an assessment of an MMRTG. The MMRTG is being used as a stand-in design, and as a standard for performance. Numerous MMRTG properties and specifications are known, and can be used as a bench-mark. By using properties of an in-use RTG we can use real design parameters, such as a desired thermal output, to review the potential of an alternatively fueled RTG.

Our work assesses the feasibility of alternate fuel sources using the SCALE-ORIGEN, and MCNP computational modeling tools for the performance of an MMRTG fueled with a different isotope than used currently by NASA. The intent of this work is to understand how a corresponding swap of the fuel source will affect performance of the most common design. Clearly, a differing isotope mass is required versus plutonium based solely on the specific decay heat of the isotopes in question, but it is not yet known how overall performance will be affected or what additional challenges to design will arise.

Since there are no alternately fueled RTGs in space missions currently, there is considerable latitude in developing research directions. Therefore, a high-level performance assessment is an apt, initial endeavor into the use of alternative fuel sources in RTGs. The scientific and technical merit of this project is to develop an understanding of the power output and density of a new RTG fuel, and if this offers acceptable performance

for current mission needs; if current configurations provide adequate shielding for potentially dangerous gamma rays, or if new fuel types warrant additional consideration in future design.

Chapter 2

Theory

2.1 Seebeck Effect

The Seebeck effect is named for Thomas Johann Seebeck, who in the early 1820s found that a junction composed of two different metals at different temperatures was able to deflect a compass [36]. He initially thought that this was a temperature induced magnetism, but determined that a "Thermoelectric Force" induced a current which deflected the compass. The temperature difference between the materials created an electrical potential which produced current in a closed circuit [37]. These junctions of dissimilar metals are called thermoelectric couples, or thermocouples (TC) for short.

This is the principle by which RTGs operate. One side of a thermocouple is heated by a radioisotope capable of some discernible decay heat, while the other side of the thermocouple is cooled by the environment. In the case of an MMRTG, the thermocouple consists of PbTe, TAGS, and PbSnTe.

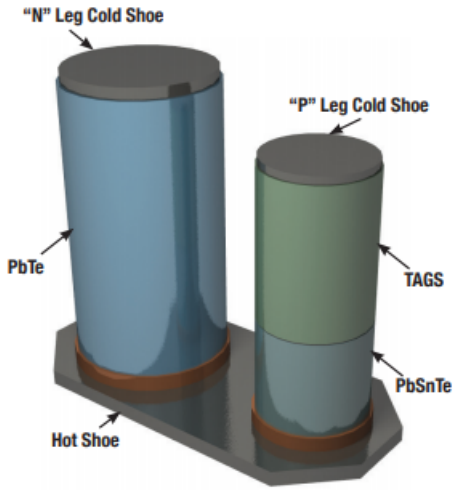

Figure 2.1: PN Thermocouple used in MMRTGs [38]

These materials have been shown to be robust over time, and are the same materials used in the Viking Mars landing crafts in 1976. For an MMRTG, the cold "shoe" is oriented to space, and the hot "shoe" towards the ^{238}Pu fuel source [38].

2.2 Radioactive Decay

Radioactive decay occurs in unstable atoms called radioisotopes. These unstable atoms emit energy through ionizing radiation. This can be through the emission of alpha particles, beta particles, gamma rays, or some combination thereof. This decay releases energy, which produces heat.

In the process of decay, the radioisotope transmutes into a decay product. This decay product is a completely different atom than the parent atom. This decay process continues until the last product is stable. But, the decay process of a specific radioisotope can occur in fractions of a second to billions of years, depending on the isotope.

In the case of an MMRTG, the fuel source is the radioisotope ^{238}Pu. This isotope decays via alpha emission, with an 87.7 year half life. ^{238}Pu produces specific decay heat of about 0.56 W/g. ^{238}Pu also has a gamma decay mode, but the energy levels are so low that they are considered negligible.

Table 2.1: Properties of selected isotopes.

Isotope	Decay Heat (W/g)	Decay Energy	Half-Life	Decay Modes
Pu-238	5.67×10^{-1}	5.593 MeV	87.7 years	$^{238}_{94}Pu \xrightarrow{\alpha} {}^{234}_{92}U$
Ac-227	3.68×10^{-2}	5.042 MeV 44.77 keV	21.7 years	$^{227}_{89}Ac \xrightarrow{\alpha} {}^{223}_{87}Fr$ $^{227}_{89}Ac \xrightarrow{\beta^-} {}^{227}_{90}Th$
Am-241	1.14×10^{-1}	5.638 MeV	432.2 years	$^{241}_{95}Am \xrightarrow{\alpha} {}^{237}_{93}Np$
Cf-252	3.88×10^{1}	6.176 MeV	2.6 years	$^{252}_{98}Cf \xrightarrow{\alpha} {}^{248}_{96}Cm$
Cm-244	2.83×10^{0}	5.902 MeV	18.1 years	$^{244}_{96}Cm \xrightarrow{\alpha} {}^{240}_{92}Pu$
Cs-137	9.23×10^{-2}	512.0 keV	30.2 years	$^{137}_{55}Cs \xrightarrow{\beta^-} {}^{137}_{56}Ba$
Po-210	1.44×10^{2}	5.407 MeV	138 days	$^{210}_{84}Po \xrightarrow{\alpha} {}^{206}_{82}Pb$
Th-228	2.68×10^{1}	5.423 MeV	1.9 years	$^{228}_{90}Th \xrightarrow{\alpha} {}^{224}_{88}Ra$
Tm-170	1.18×10^{1}	968.3 keV 314.0 keV	129 days	$^{170}_{69}Ac \xrightarrow{\beta^-} {}^{170}_{70}Yb$ $^{170}_{69}Ac \xrightarrow{\epsilon} {}^{170}_{68}Er$

The radioisotopes that are reviewed for potential Plutonium-238 replacement are Actinium-227, Americium-241, Californium-252, Curium-244, Polonium-210, Thorium-228, and Thulium-170. See Table 2.1 for decay modes, and properties of the isotopes to be reviewed. These radioisotopes were all chosen because they have moderate half-lives and have decay heat with the potential to power a RTG. Many other isotopes were reviewed and rejected due to their decay modes, low decay-heat, or too short half-lives.

Ac-227 is currently being produced as a precursor to Ra-223 which is used to treat prostate cancer. As such, extraction methods are known. Source material for Ac-227 begins with the recovery of Ra-226 for legacy medical devices, so it can be assumed that supply is limited. Ra-226 is purified and then small targets are irradiated in the High Flux Isotope Reactor. This requirement of high flux makes production difficult.

Am-241 is currently increasing in availability due to the decay of depleted nuclear fuel, specifically the beta decay of Pu-241. Technology for extraction has been well vetted in the UK, but is not available in the USA.

Cf-252 can only be produced in two reactors in the world. Cf-252 begins with Berkelium-249 targets. This material is reactor produced. Berkelium-249 targets are bombarded with neutrons to form Berkelium-250. This decays to Cf-250, two additional neutron captures result in Cf-252. Cf-252 is subsequently purified.

Curium is formed in a nuclear reactor through neutron capture and beta decay reactions. Curium 244 accumulates over time, and can be available in abundance. With an 18 year half-life, reactor produced Cm-244 in reactor fuel is decreasing over time. Cm-244 could also be produced in the HFIR with processing. Cm-244 is potentially abundant through reprocessing nuclear fuel, but the US does not reprocess used nuclear fuel.

Cesium-137 is produced spontaneously through fission. Numerous techniques have been developed for separation of Cs-137 from other fission products.

Polonium 210 is produced via neutron irradiation of Bismuth 209. The source material is essentially natural bismuth, and available. The need for irradiation, short half-life,

toxicity and volatility of Po-210 makes processing post irradiation very difficult.

Th-228 can be produced by the successive neutron capture and beta decay of Ra-226. Ra-226 exists as the sixth member of the U-238 decay chain, and is not overly abundant. There is not much information available on purification techniques for this isotope, but it can be assumed from the short half-life and intense decay heat that processing would be difficult.

Tm-170 can be produced in medium flux reactors through thermal neutron bombardment of Thulium 169, essentially natural Thulium. Unfortunately, the source material, natural thulium, is the least abundant of the rare-earth elements. Production scale of Tm-170 for radioisotope power systems has been considered in the past, so doing so is not a new concept.

Chapter 3

Method

3.1 SCALE-ORIGEN

Oak Ridge Isotope Generation (ORIGEN) is a general purpose, point depletion and decay code. It has been developed to calculate isotope concentrations, decay heat, radiation source terms, and curie levels. This code calculates time-dependent concentrations, along with activities and radiation source terms for numerous isotopes generated and depleted with neutron capture, fission, and radioactive decay, as well as other uses. ORIGEN data libraries are based on ENDF/B-VII.1 and JEFF-3.0/A evaluations, and include nuclear decay data, neutron reaction cross sections, neutron-induced fission product yields, delayed gamma emission data, and neutron emission data for over 2,200 nuclides. Photon yield libraries are based on recent ENSDF nuclear structure evaluations, and contain discrete line energy and intensity data for decay gamma-ray and x-ray emission for 1,132 radionuclides. Decay data includes all ground and metastable nuclides with half-lives greater than one millisecond.

3.1.1 ORIGEN Decay

ORIGEN solves the system of ordinary differential equations describing nuclide generation, depletion and decay:

$$\frac{dN_i}{dt} = \sum_{j \neq i} (l_{ij}\lambda_j + f_{ij}\sigma_j\phi)N_j(t) - (\lambda_i + \sigma_i\phi)N_i(t) + S_i(t) \tag{3.1}$$

Where N_i = atoms of nuclide "i"

λ_i = decay constant (1/s) of nuclide "i"

l_{ij} = fractional yield of nuclide "i" from decay of nuclide "j"

σ_i = spectrum-averaged removal cross section (barn) for nuclide "i"

f_{ij} = fractional yield of nuclide "i" from neutron-induced removal of nuclide "j"

Φ = angle and energy-integrated time-dependent neutron flux (n/cm^2-s)

S_i = time dependent source term (atom/s)

There is no spatial dependence in this equation, and as such can be interpreted as either a solution for a point in space, or a spatial average over a volume. This second solution is the one used in this study. With this, Φ becomes the spatially averaged neutron flux magnitude, with energy-dependence embedded in the one-group flux weighted average cross sections σ_i and reaction yields f_{ij}. In matrix form, Eqn. 3.1 can be written as:

$$\frac{d\vec{N}}{dt} = \mathbf{A}\vec{N}(t) + \vec{S}(t) \tag{3.2}$$

Where $\mathbf{A}$ is referred to as the transition matrix, and is represented by:

$$\mathbf{A} = \mathbf{A}_\sigma \Phi + \mathbf{A}_\lambda \tag{3.3}$$

Where $\mathbf{A}_\sigma$ contains the reaction terms, and $\mathbf{A}_\lambda$ contains decay terms. This is convenient, for numerical solutions over step n hold reaction, flux, and feed terms constant:

$$\frac{d\vec{N}}{dt} = (\mathbf{A}_{\sigma,n}\Phi_n + \mathbf{A}_\lambda)\vec{N}(t) + \vec{S}_n \tag{3.4}$$

$$Over\ t_{n-1} \leq t \leq t_n$$

ORIGEN can compute the alpha, beta, neutron, and gamma emission spectra during decay through:

$$R_x^g(t) = \sum_i \lambda_i N_i(t) \int_{E^g}^{E^{g-1}} w_{i,x}(E)dE \tag{3.5}$$

Where $w_{i,x}$ is the number of particles of type x emitted per disintegration of nuclide "i" at energy "E", using energy bins defined from E^g to E^{g-1}, where "g" is an index.

While ORIGEN is capable of computing spectra for alpha, beta, neutron, and gamma spectra, gamma is the primary spectra of concern for this work. ORIGEN calculates the total photons from decay of nuclide "i" with:

$$Y_{i,\gamma} = \frac{\lambda_{i,\gamma}}{\lambda_i} \tag{3.6}$$

Where the right-hand of the equation is the fraction of decays emitting photons. Photons emitted by nuclide "i" at energy level "E" is given with:

$$w_{i,\gamma}(E) = Y_{i,\gamma} X_{i,\gamma}(E) \tag{3.7}$$

Where the spectrum $X_{i,\gamma}(E)$ is fundamental data, including line data from x-rays, and gamma-rays, continuum data from bremsstrahlung, spontaneous fission gamma rays, and gamma rays from (α, n) reactions, with bremsstrahlung data having been tabulated rather than calculated. This feature was used in this study to determine gamma spectra over time for radionuclides.

3.1.2 ORIGEN Decay Heat

SCALE is also capable of calculating decay heat for a nuclide, or group of nuclides over time. This is an especially important feature for the study of potential radionuclides for use in RTG's. SCALE performs this calculation via:

$$H_z = \sum_{i=1}^{itot} Q_i \lambda_i \frac{M_Z^{(i)}}{A^{(i)}} \cdot 1.602 \times 10^{-13} \cdot N_A = 9.65 \times 10^{10} \sum_{i=1}^{itot} Q_i \lambda_i \frac{M_Z^{(i)}}{A^{(i)}} \tag{3.8}$$

Where Q_i = the decay energy of nuclide "i" in MeV

λ_i = the decay constant of nuclide "i" in 1/s

$M_Z^{(i)}$ = mass of nuclide "i" in zone "Z" in grams

$A^{(i)}$ = mass of one mole of nuclide "i" in grams

$itot$ = total number of nuclides

1.602×10^{-13} = conversion factor of MeV to joules

3.2 MCNP

Due to the complexities from materials and geometry specifications in a full-scale MMRTG model, it was determined that radiation transport would be best performed through Monte Carlo methods in MCNP6, as other potentially useful probabilistic radiation transport software may not have the capability of handling the complex geometries required for this work [39].

MCNP6 is a general-purpose, continuous-energy, generalized-geometry, time-dependent Monte Carlo radiation-transport code designed to track many particle types over broad ranges of energies. The code can treat arbitrary three-dimensional configurations of materials in geometric cells [8]. MCNP6 has numerous applications in the fields of nuclear science and engineering, from nuclear reactor design to medical physics.

For photon transport, this code accounts for coherent and incoherent scattering of photons, the potential for fluorescent emissions after photoelectric absorption, and absorption in electron-positron pair production.

MCNP can utilize several transport modes including neutron only, photon only, electron only, combined neutron/photon transport where photons are produced by neutron interactions, neutron/photon/electron, photon/electron and electron/photon. In MCNP, photons are capable of energies between 1 keV and 100 GeV. MCNP input cards require a geometry specification, including the specification of materials and densities. Physics which can specify energies, source terms, and particles to be tracked, are also required. Additionally, MCNP inputs provide for desired output forms and tallies, and variance reduction techniques.

Monte Carlo techniques model problems by simulating the behavior of individual particles and tallying average behavior. This is significantly different from deterministic transport methodologies which solve transport equations for average particle behavior.

For Monte Carlo methods, average behavior of particles in a system is inferred. And, while deterministic methods provide solutions for numerous aspects and parts of a system, in MCNP only specific solutions are found through predetermined tallies. That said, Monte Carlo is good at solving complex, three-dimensional, time-dependant problems. Monte Carlo does not use averaging approximations in terms of space, energy, and time.

3.3 MMRTG

One of the major initial requirements for this project was the development of an RTG model in MCNP. As the current United States space program RTG model is the MMRTG, the focus for initial model development is based on this design. This gives both a geometric model, and a goal of 2000 watts thermal power [38] for an output of an alternative source.

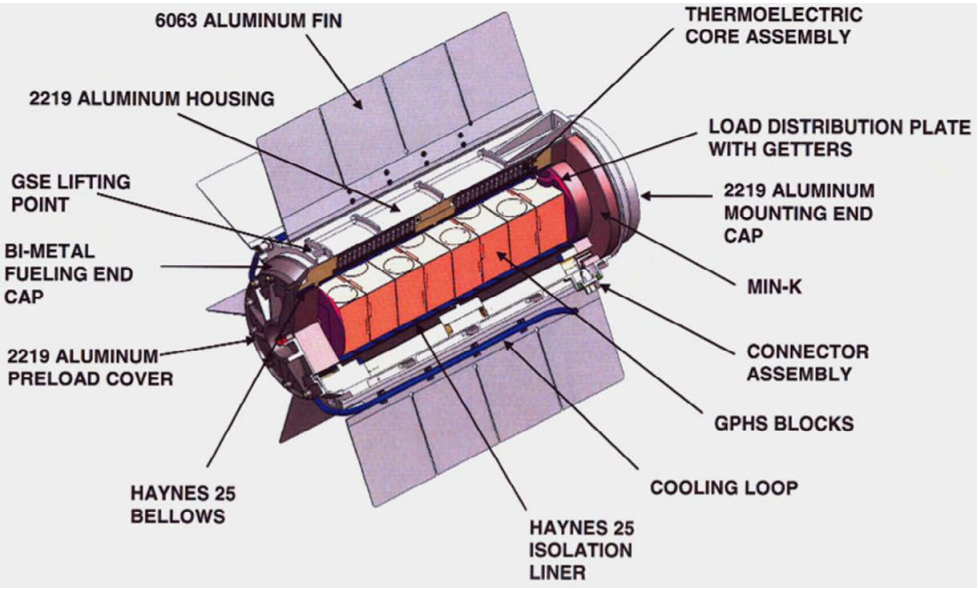

Figure 3.1: MMRTG with select materials [40].

Much of the information on specifications and design criteria for the MMRTG is export controlled, and therefore unavailable. As such, it has been necessary to locate secondary sources so as to make estimations and generate the information needed to

build a suitable MMRTG model in MCNP for this feasibility analysis.

3.3.1 GPHS Model Design

The General Purpose Heat Source (GPHS) contains the powerhouse of contemporary NASA RTG's. These are stackable, and in the case of the GPHS-RTG these were configurable for particular power outputs desired. The MMRTG design utilizes a stack of eight GPHS units, fueled with Pu-238, to achieve a desired power output. The potential for the return from orbit, or launch abort exists for any space mission. As such, the heat source for any RTG must be contained by a series of physical barriers robust enough to withstand the failure of a mission launch, or return to earth's surface through the atmosphere. This is an important design consideration for future work, as a great effort must be made in designing modules both capable of containing a new fuel source, and robust enough to withstand reentry.

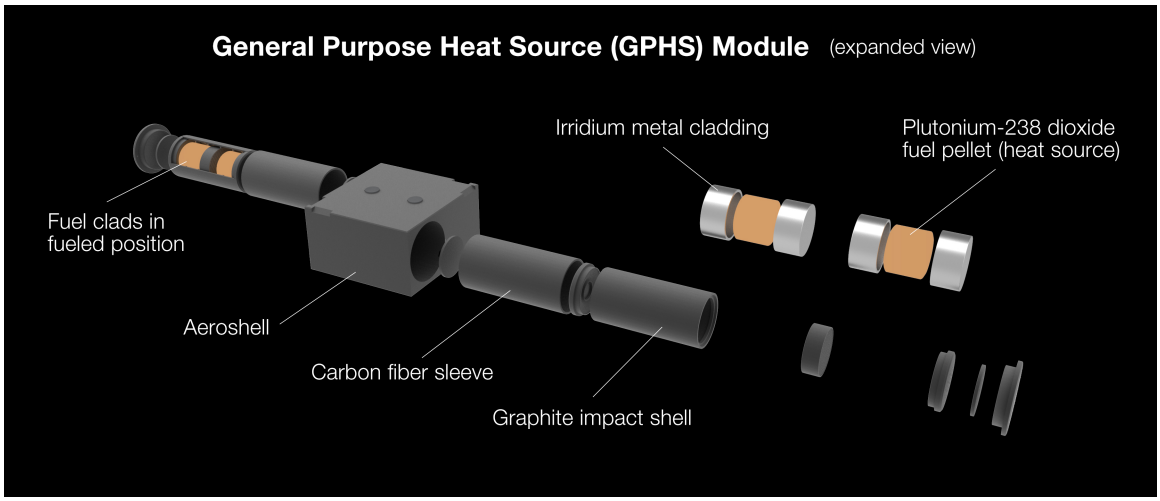

Figure 3.2: NASA rendering of expanded GPHS [41].

GPHS geometries and specifications used to fuel contemporary RTG's were determined from design studies [42], [43]. Fuel pellets are encased in iridium shells. These capsules are located within a Fine Weave Pierced Fabric (FWPF) impact shell, which is located within a Carbon Bonded Carbon Fiber (CBCF) thermal insulation, within another FWPF shell [43]. These are all contained within a Poco Graphite AXF-5Q1

aeroshell.

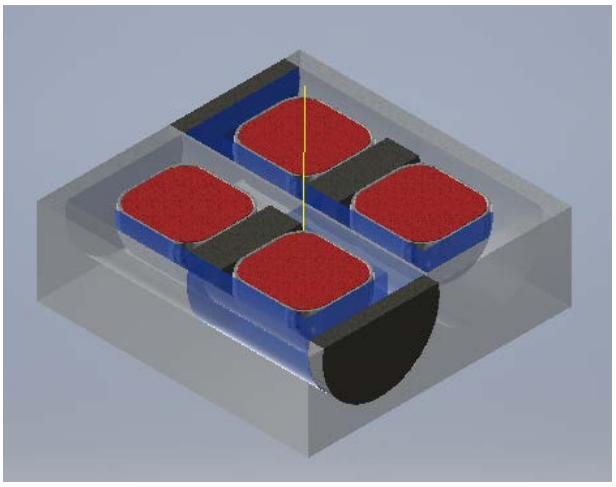

Figure 3.3: CAD rendering of GPHS, with estimated dimensions.

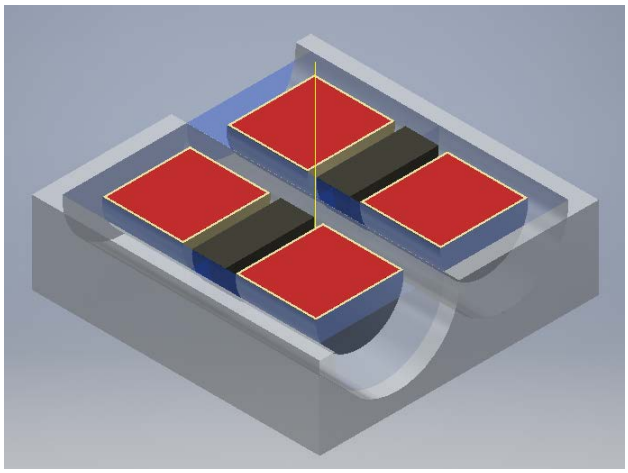

Figure 3.4: CAD rendering of GPHS, with geometry as used in MCNP model.

3.3.2 MCNP Model Design

Due to the nature of MCNP's geometry input, certain simplifications were made. Fillets within the GPHS have been neglected for the sake of geometric simplicity. The length of the cylindrical pellets was modified to maintain the mass of the active material with the diameter of the pellets remaining constant. Thicknesses for the iridium clad, and carbon shells were maintained in accordance with previously determined specifications. Fuel pellets were modeled in MCNP as either plutonium dioxide, or Am-241 oxide.

Thermocouple (TC) arrays have been modeled with homogeneous materials in the full MMRTG rather than having each shoe with its correct, discrete material composition. Because of this simplification, an additional study was performed to compare the gamma flux through homogeneous and non-homogeneous TC arrays outside the scope of an MMRTG. Figure 3.5 shows a cross-sectional view of the TC array geometry as developed in MCNP, and visualized in VisEd [44].

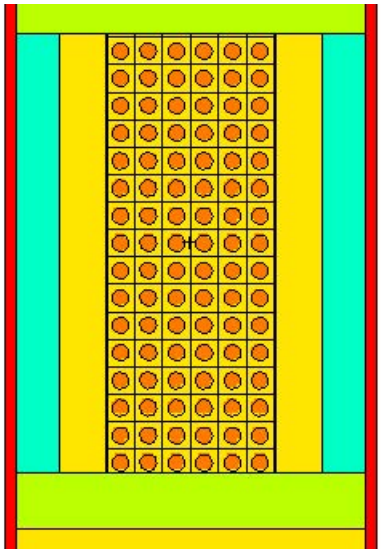

Figure 3.5: Visualization of side-cross section of TC array as developed in MCNP6. Colors indicate differing materials.

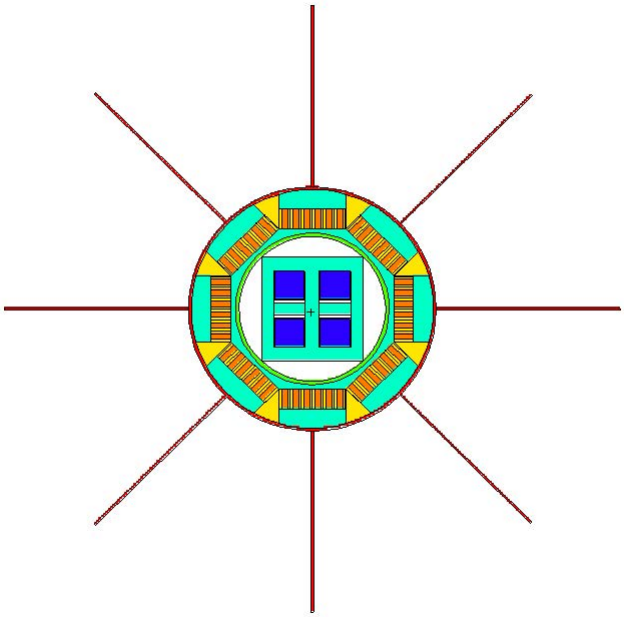

Figure 3.6: Visualization of top-view of MMRTG as developed in MCNP6. Colors indicate differing materials.

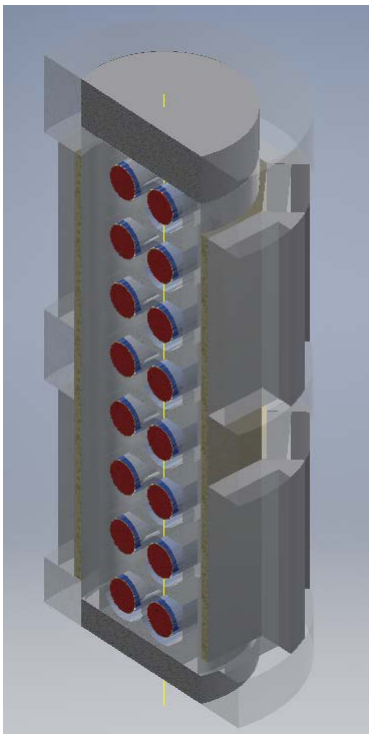

Figure 3.7: CAD rendering of geometry utilized in MCNP model. Exterior surfaces and fins are neglected in this rendering, but utilized in MCNP model.

Dimensions for the MMRTG itself are export controlled. It has been necessary to

Table 3.1: Properties of selected materials.

Material	Composition	Density (kg/m^3)
Haynes-25	Co, Ni, Fe, Cr, Mo, W, Mn, Si, C	9070 [46]
Min-K TE1400	Si, TiO_2	320 [47]
Microtherm Super G	Al_2O_3	320 [48]
Poco Graphite AXF-5Q1	Carbon	1742 [49]
DOP-26	Ir, W, Th, Al [50]	2265

make assumptions on the dimensions of the MMRTG based on scale renderings of the MMRTG [32] and geometry of the GPHS for scale [45]. While fins on the exterior of the MMRTG have a negligible impact on initial investigations of radiation transport, these were included in the model to provide a sense of scale, see Figure 3.6.

Material properties for the MCNP model have been compiled through various sources. Compositions and densities of individual components were determined or estimated through reports from manufacturers, studies, or book chapters. While best engineering judgments were made as to the compositions, this topic remains a vulnerability of this study, as small changes in material compositions can have large impacts on radiation transport behavior.

Chapter 4

Results

4.1 Heat Production

Decay heat rates for the isotopes reviewed were produced using SCALE-ORIGEN. SCALE inputs required bounds and specifying the radiation of interest. This also included the material used and specifications of libraries. It was also necessary to bound the decay outputs by a time scale, with particular time steps. Outputs included nuclide generation, gamma spectra, and specific decay heat. Each of these parameters was given for every time step and saved. Different cases for the the various isotopes required small adjustments to input files, which was mainly for the windows for data generation. If isotopes generated no data for low or high energy bins, these bins were stripped from the inputs, and codes were run again. If it was apparent that several energy peaks were being lost in energy bins which were too coarse, or cut off too early, bin spacing was made finer, or windows were made larger, and codes were run again. Data from output files was converted to comma-separated data files. These were fed into Python 3 for visualization. Following this method, both heat profiles and gamma spectra were generated for all isotopes in question. See Appendix A for an example input case for Am-241 in SCALE-ORIGEN.

Pu-238 shows an approximately linear heat profile over its lifetime. It is straightforward to see how the heat profile of Pu-238 would provide a robust lifespan. The predictability of the isotope provides for design parameters easier to accommodate than those of isotopes that were reviewed in the past. The specific decay heat lost for Pu-238 is small compared with other isotopes, as can be seen in Figures 4.4, and 4.7.

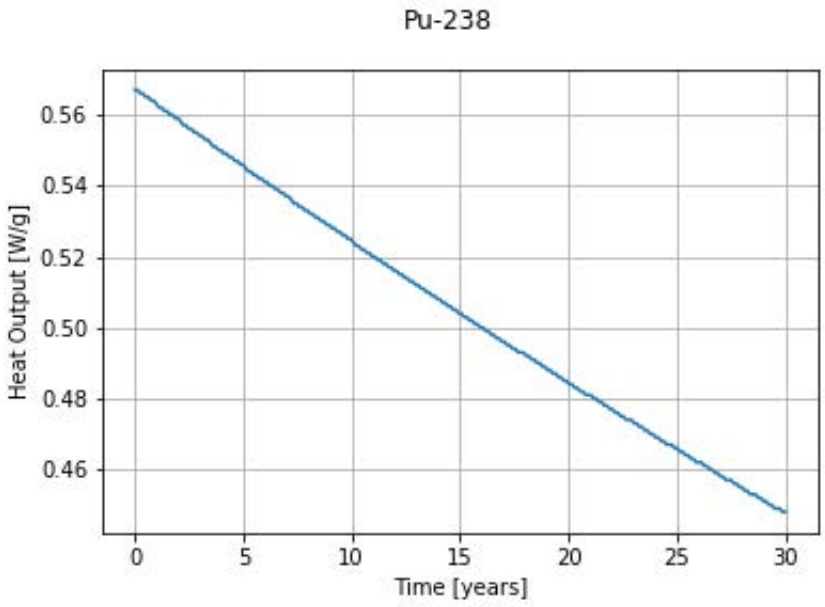

Figure 4.1: Specific decay heat of Pu-238 over thirty years.

Of the isotopes reviewed, Th-228, Cf-252, Po-210, and Tm-170 exhibited the most unstable heat-output over the potential life of an MMRTG, with initially high heat decaying significantly over 30 years. Each of these isotopes had W/g decreases of several orders of magnitude. Po-210 and Tm-170 demonstrated the greatest vulnerabilities in terms of heat output, losing the majority of their useful decay heat output in about a year. Th-228 and Cf-252, while more robust than Po-210 and Tm-170, had a significant decrease in decay heat over the first five, providing a very uneven heat profile over the design life of an MMRTG.

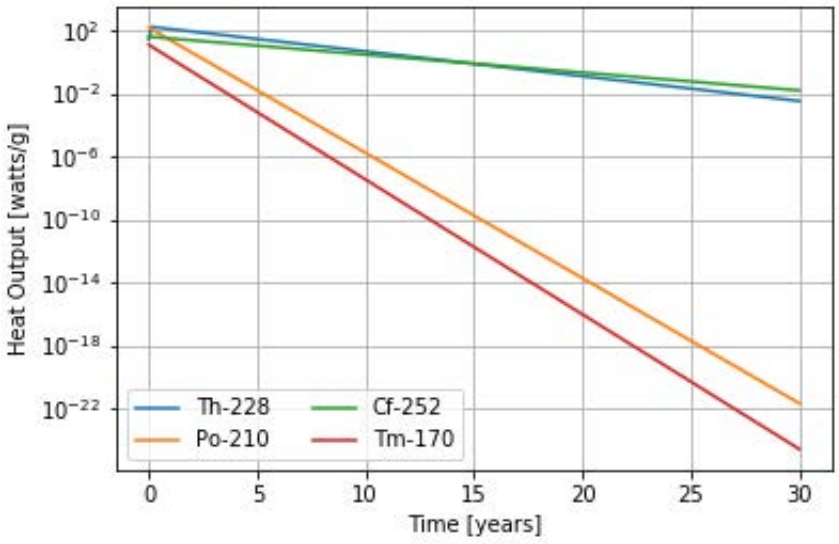

Figure 4.2: Specific decay heat of Th-228, Cf-252, Po-210, and Tm-170 over thirty years.

Ac-227, Am-241, Cm-244, and Cs-137 have the more stable heat profiles across 30 years. While Ac-227, Am-241, Cm-244, and Cs-137 decay heats are reduced by less than an order of magnitude each, Ac-227 drops from a peak of slightly greater than 14 W/g to 6 W/g. Additionally, Ac-227 has very little decay heat initially, with the majority of its heat output due to numerous short-lived daughter products, see Figure 4.3. Ac-227 decays via β^- to Th-227. Likewise, Cs-137 begins with a low heat output, but peaks at about 0.42 W/g due to β^- decay to Ba-137m and drops to about 0.21 W/g by the end of 30 years.

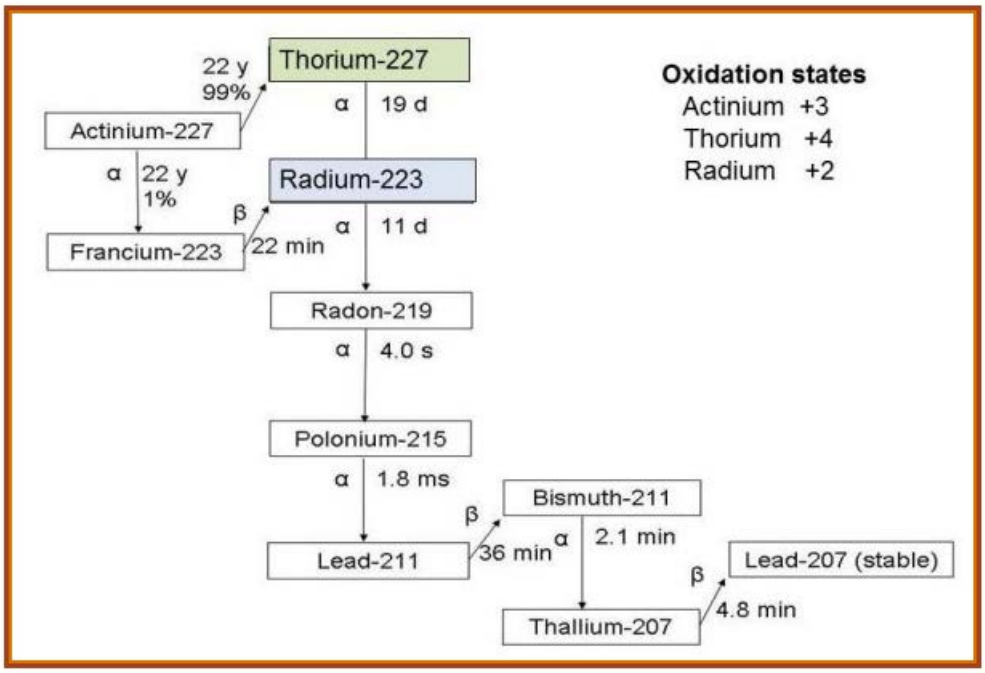

Figure 4.3: Decay Chain of Ac-227 [51].

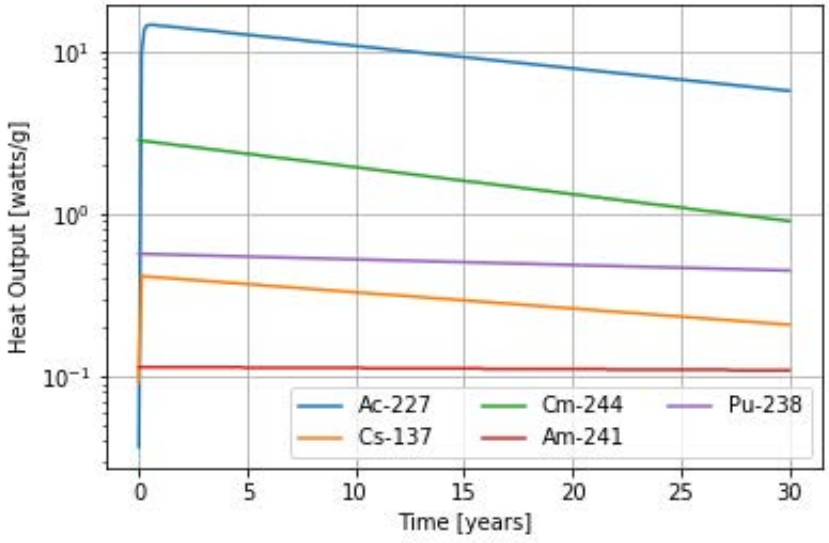

Figure 4.4: Specific decay heat of Ac-227, Cm-244, Cs-137, and Am-241 over thirty years, with Pu-238 for comparison.

For stable useful heat over the life of an MMRTG, the least stable of this group are Ac-227, Cs-137, and Cm-244. Of these moderately stable isotopes, Cm-244 appears to have the most promising profile. This radioisotope begins with about 2.8 W/g specific

decay heat, and drops to below 1 W/g after 30 years. While this is a significant reduction in heat output, it provides a good initial profile, with moderate stability over time. Cm-244 has an unfavorable output of neutrons which would require additional shielding, see Figure 4.19. Of the three aforementioned isotopes, none appear to be nearly as stable as Pu-238.

Of all the isotopes reviewed, Am-241 has the lowest peak decay heat, at 0.117 W/g. The next lowest decay heat/isotope is Cs-137, which after 30 years still has a greater heat output than that of Am-241 at its 0 year value. While the low specific heat is a vulnerability, Am-241 boasts the most stable heat output of all the isotopes reviewed, decreasing by less than 0.01 W/g over thirty years. It has the most apparent linear heat output of all the radioisotopes reviewed, including Pu-238, as can be seen in Figures 4.5 and 4.6. The consistency of the available heat for Am-241 demonstrates the potential for a significantly longer design life of an americium fueled RTG, vs. a conventional plutonium fueled device.

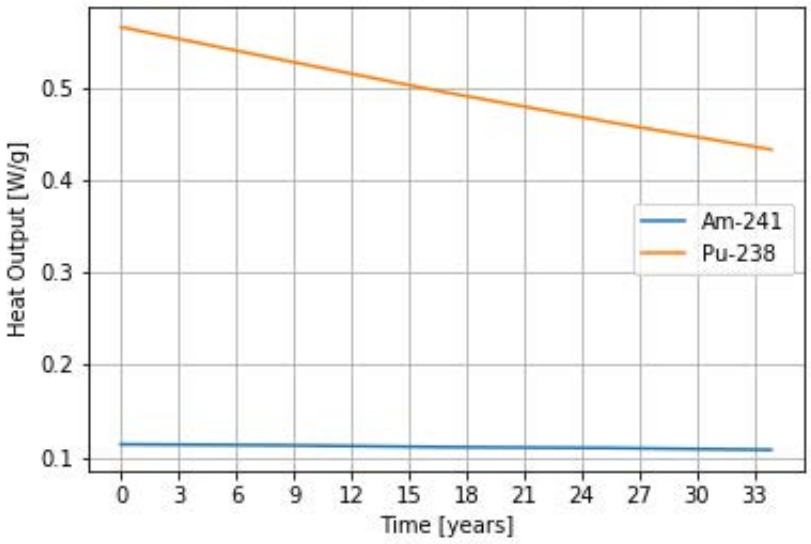

Figure 4.5: Comparison of specific decay heat for Am-241 and Pu-238 over approximately 33 years.

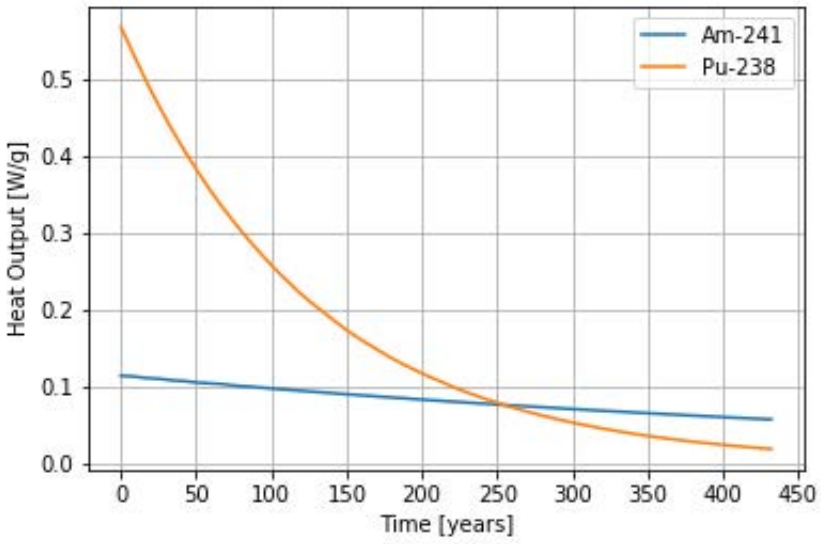

Figure 4.6: Comparison of specific decay heat for Am-241 and Pu-238 over the half life of Am-241.

Table 4.1: Properties of selected isotopes, with potential chemical forms, approximate densities of said forms, adjusted heat outputs, and required mass and volume for 2000 W of thermal power.

Isotope	Chemical Form	Density (g/cm^3)	Adjusted Heat (W/cm^3)	Required Mass (g)	Required Volume (cm^3)
Pu-238	PuO_2	11.5	3.75	4,001	347
Ac-227	Ac_2O_3	9.18	0.31	60,000	6,546
Ac-227[1]			120.38	152	16.6
Am-241	Am_2O_3	11.7	1.21	19,290	1,648
Cf-252	CfO_2	12.69	436	58	4.6
Cm-244	Cm_2O_3	12.17	31	778	63.9
Cs-137	CsCl	3.99	0.29	27,267	6,834
Cs-137[1]			1.31	6,094	1,527
Po-210	$PoCl_2$	6.5	700	18.6	2.8
Th-228	ThO_2	10	235	85	8.5
Tm-170	Tm_2O_3	8.6	85	201	23

Table 4.1 provides properties derived for the isotopes reviewed in this study. Given values for densities are widely available. The adjusted heat value is found by multiplying initial specific decay heat by the density of the chemical form, with heat inputs weighted by the the mass of radioisotopes. Required mass was determined by dividing the specific

thermal heat requirement of an MMRTG by the adjusted heat value. This gave required volume. This required volume was then multiplied by density to determine the required mass. Peak values indicate the analysis of a radioisotope using its peak specific heat, rather than its initial value. This was necessary for isotopes that decayed into hotter daughter products than the initial parent. This provided a preliminary demonstration of the value of Ac-227, Cf-252, Cm-244, Po-210, Th-228 and Tm-170. The chemical form for each of these isotopes require less mass, and less volume to achieve the same heat output as Pu-238. Although, Po-210 and Tm-170 have very unstable heat profiles. Th-228 and Cf-252 have slightly more linear heat outputs, but compared to the stability of Pu-238, these radioisotopes do not have favorable properties for long-term use, see Figure 4.7.

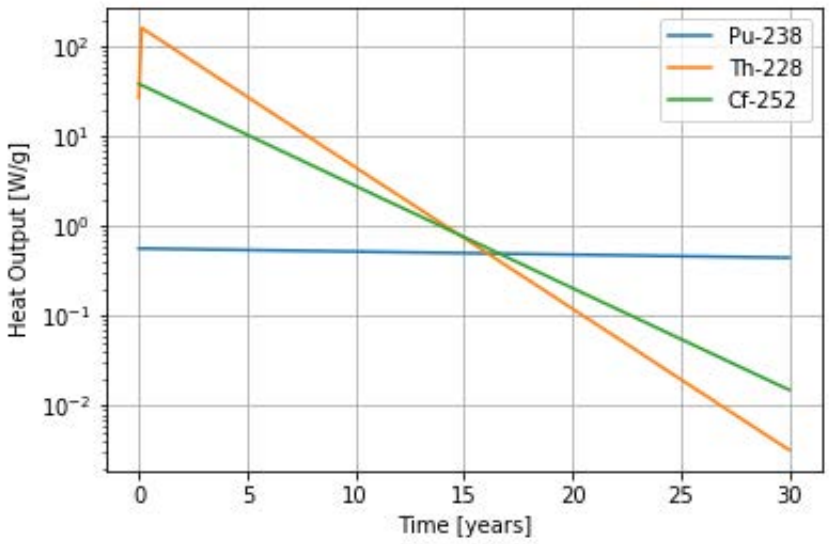

Figure 4.7: Comparison of heat outputs for Pu-238 to Th-228 and Cf-252.

Of the remaining isotopes, Am-241 and Cs-137, required masses are quite different. Am-241 may require 19 kg, at about 1600 cm^3, while Cs-137 could require 6 kg, at 1500 cm^3. This differing condition between the radioisotopes volume and mass is due to the

[1]Values for peak heat production. An increase in activity occurs after the initial formation of the isotope, showing that decay products increase the value of these heat sources, see figure 4.4. As such, it was prudent to review isotopes according to their potential output, rather than initial output.

specific decay heat, and density of the fuel forms.

The calculated mass requirement for Pu-238 is somewhat less than the actual 4.8 kg amount specified by NASA [38]. This variability is due to the actual composition of the plutonium fuel, which would already include daughter products and other impurities. Initial comparisons have been done with pure Pu-238, as purity in the composition of other radioisotopes was assumed. Radiation transport will reflect more reasonable fuel compositions [52].

4.2 Safety

4.2.1 Gamma Radiation

Using the same code for decay heat, gamma spectra for isotopes were developed through SCALE-ORIGEN. SCALE inputs required bounds and specifying the radiation of interest. This also included the material used and specifications of libraries. It was also necessary to bound the decay outputs by a time scale, with particular time steps. Outputs included nuclide generation, gamma spectra, and specific decay heat. Each of these parameters was given for every time step, and saved. Different cases for the the various isotopes required small adjustments to input files. This was mainly for the windows for data generation. If isotopes generated no data for low or high energy bins, these bins were stripped from the inputs, and codes were run again. If it was apparent that several energy peaks were being lost in energy bins which were too coarse, or cut off too early, bin spacing was made finer, or windows were made larger, and codes were run again. Data from output files was converted to comma-separated data files. These were fed into Python 3 for visualization. Following this method, both heat profiles and gamma spectra were generated for all isotopes in question. See Appendix A for an example input case for Am-241, in SCALE-ORIGEN.

The majority of isotopes reviewed are alpha emitters, with a few undergoing beta decay. While neutrons are of concern, this will be addressed later. This data required

another small modification to the SCALE-ORIGEN input files to add the generation of neutrons to outputs.

Most of these isotopes emit gamma radiation through radioactive decay at various energy levels. While the majority of the heat output for each isotope is due to the energy level of alpha and beta emissions, trends for energy from gamma emission closely follow that of heat output. This can be seen through a comparison of Figures 4.8 and 4.2, as well as Figures 4.4 and 4.9.

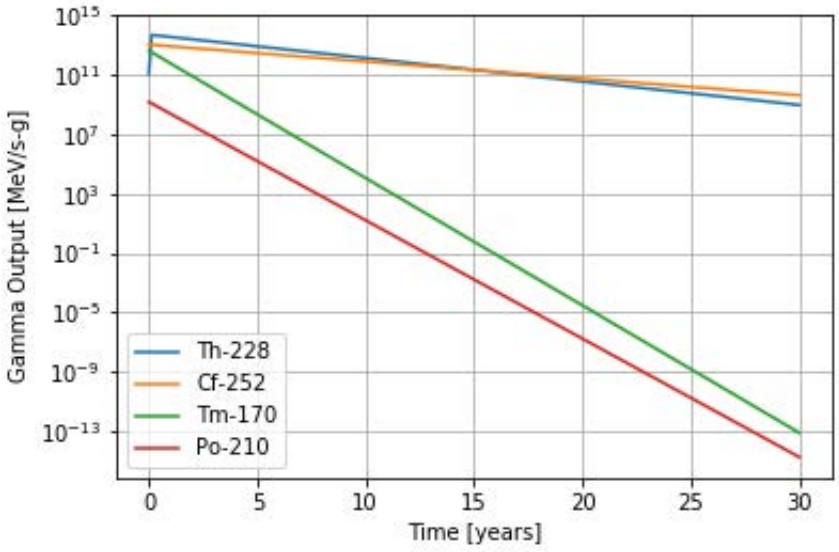

Figure 4.8: Specific gamma output of Th-228, Cf-252, Tm-170, and Po-210 over 30 years.

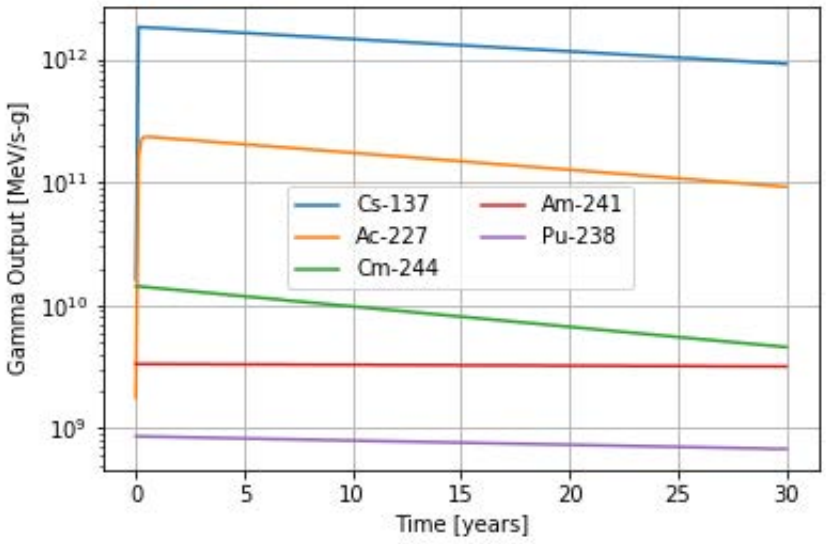

Figure 4.9: Specific gamma output of Cs-137, Ac-227, Cm-244, Am-241, and Pu-238 over 30 years.

The gamma spectrum of each isotope provides high-level information on needs for gamma shielding. Pu-238 has a gamma peak near 2 E-02 MeV, with an output of 8.64 E08 MeV/s-g demonstrating that the majority of contributions are due to low-energy gammas (Figure 4.10).

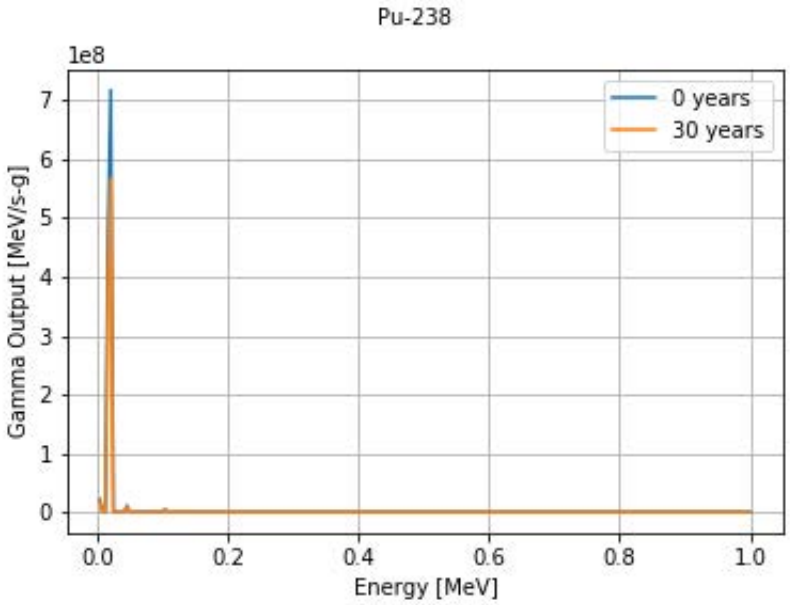

Figure 4.10: Gamma Spectra of Pu-238 for 0 and 30 years of life.

Several of the isotopes reviewed have significant changes to their gamma emissions over thirty years, beyond a decrease in energy. Ac-227, Cs-137, and Th-228 readily decay to products with significantly higher gamma emissions than the parent isotope. Within the first year of life, Th-228 has a significant increase in total energy produced, as well as in the energy of the gammas emitted (Figure 4.13). Between one and thirty years, the output decreases by nearly five orders of magnitude (Figure 4.14).

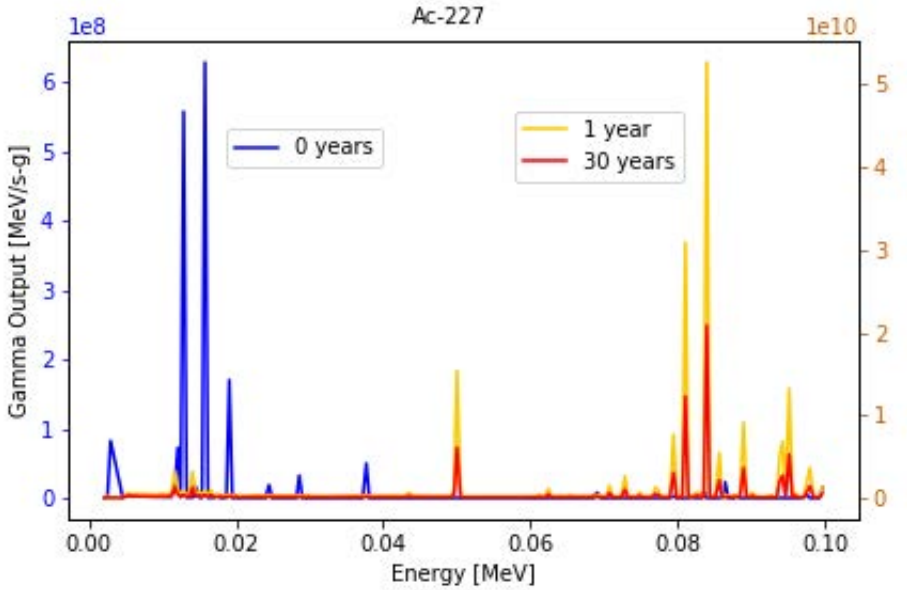

Figure 4.11: Gamma Spectra of Ac-227 for 0 to 30 years of life.

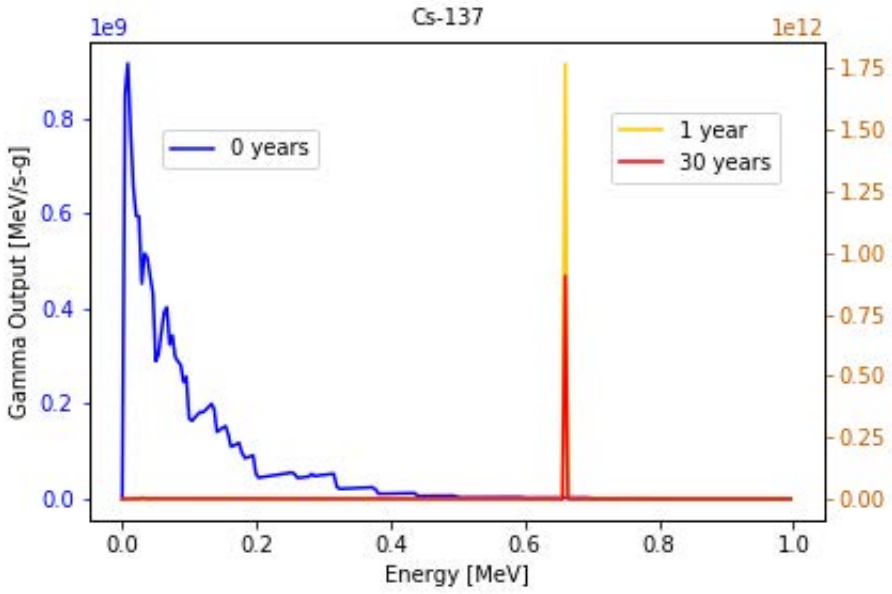

Figure 4.12: Gamma Spectra of Cs-137 for 0 to 30 years of life.

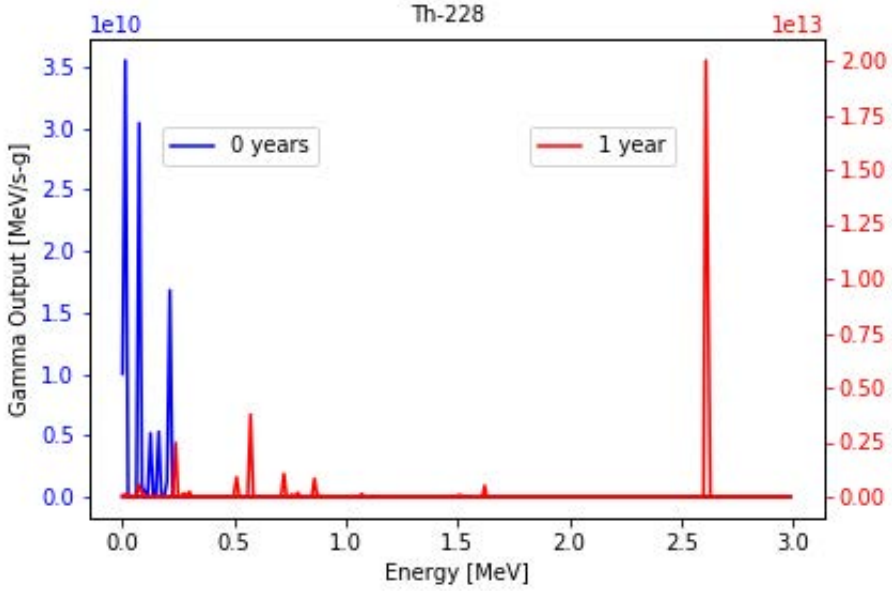

Figure 4.13: Gamma Spectra of Th-228 for 0 and 1 year of life.

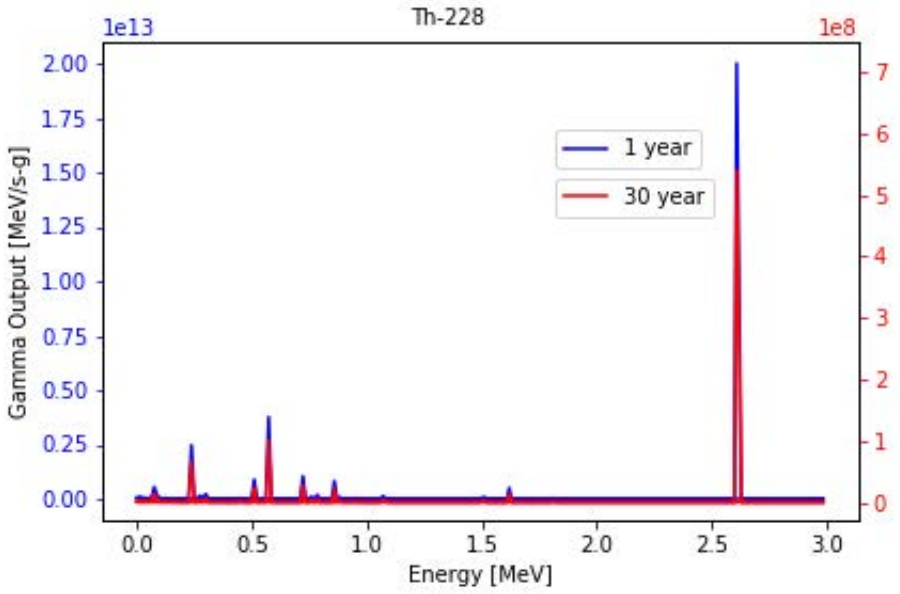

Figure 4.14: Gamma Spectra of Th-228 for 1 and 30 years of life.

Of all the isotopes reviewed, Cf-252 has the broadest spectrum, with significant contributions between approximately zero and five MeV (Figure 4.15). This has a maximum of approximately 5.67 E11 MeV on a 1 gram basis. With the broad values, Cf-252 has a total output near 9.85 E12 MeV/s-g. This decreases significantly over thirty years to 3.98 E9 MeV/s-g.

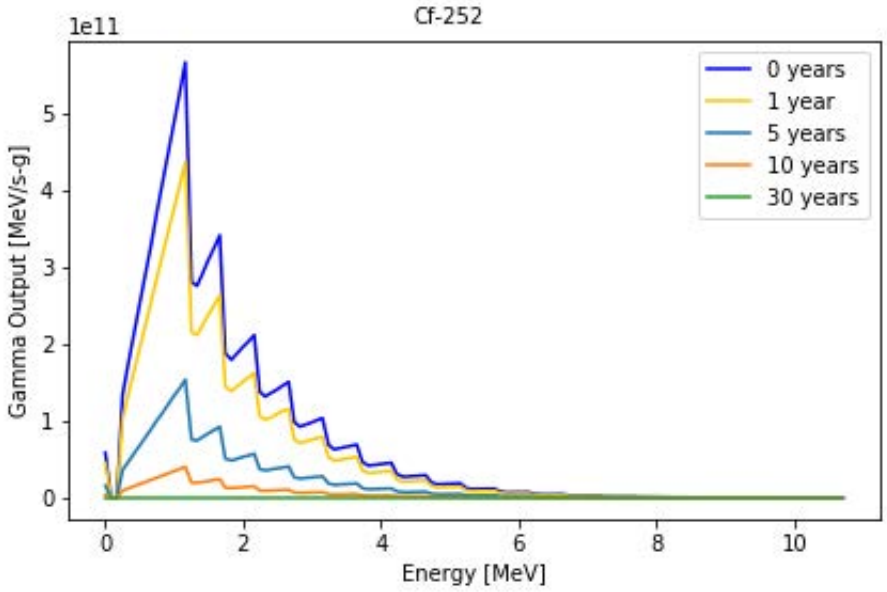

Figure 4.15: Gamma Spectra of Cf-252 for 0 to 30 years of life.

Polonium-210 has the lowest rate of gamma emission rate per unit mass for all isotopes reviewed. Of all other isotopes considered, Po-210 has the closest value to Pu-238, at 1.40 E09 MeV/s-g to 8.64 E08 MeV/s-g, respectively, but dipping below Pu-238 output within a year.

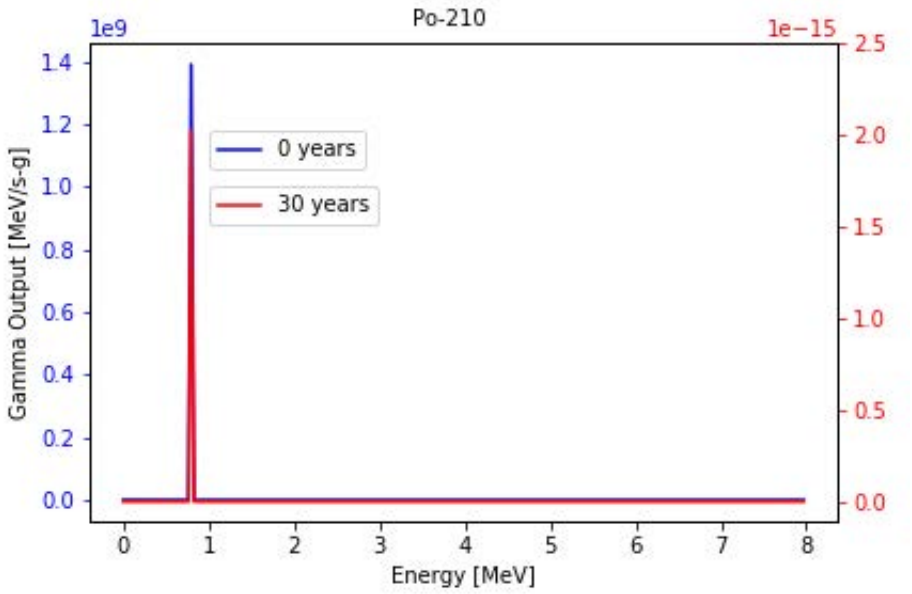

Figure 4.16: Gamma Spectra of Po-210 for 0 and 30 years of life.

Americium 241 has the second lowest maximum rate of gamma emission per unit mass at 3.44 E09 MeV/s-g. It has the most stable output over 30 years, decreasing by only 1.5 E08 MeV/s-g.

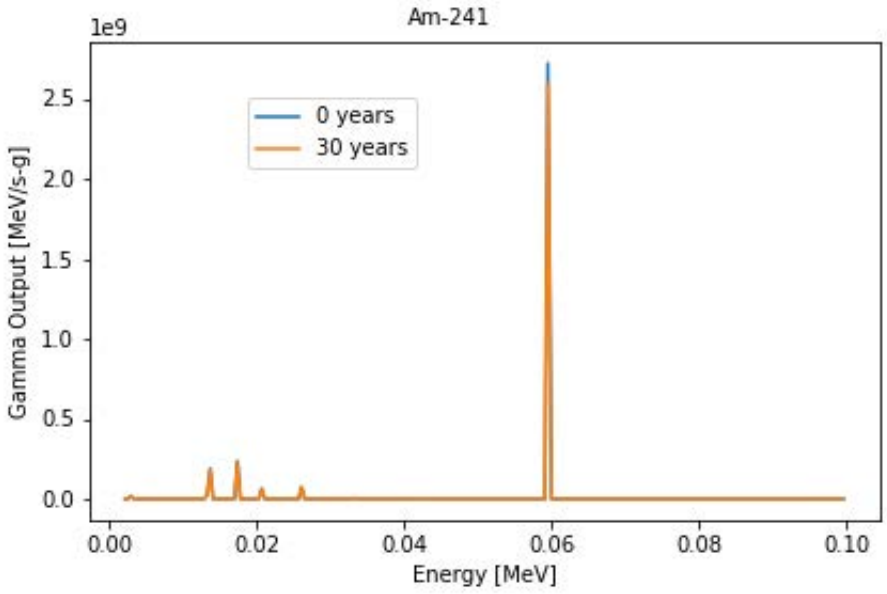

Figure 4.17: Gamma Spectra of Am-241 for 0 and 30 years of life.

Tm-170 produces relatively low energy gammas, but even so, emits 3.86 MeV/s-g. This value drops steadily over thirty years by over 25 orders of magnitude.

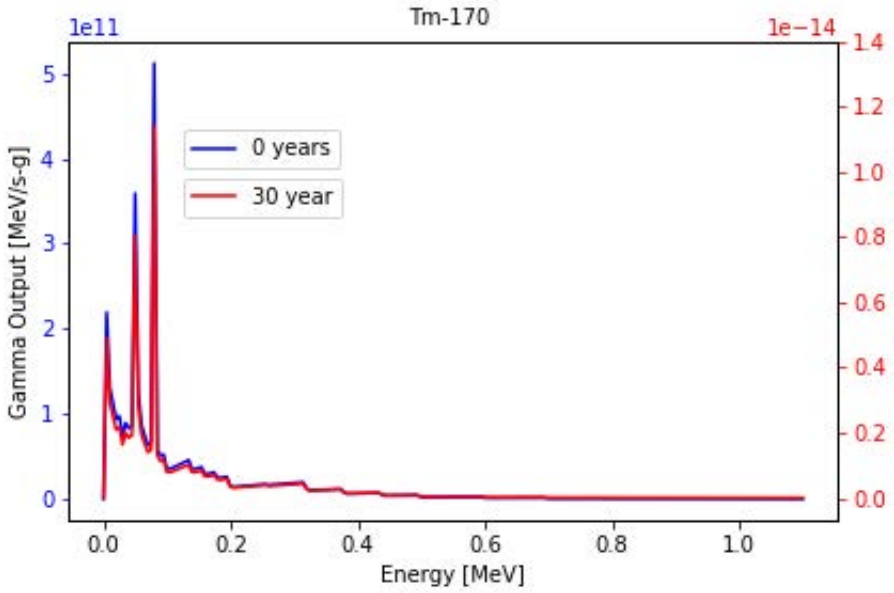

Figure 4.18: Gamma Spectra of Tm-170 for 0 and 30 years of life.

4.2.2 Preliminary Selection

Isotopes have been assessed through their relative heat output, stability of heat output, and required mass. Additionally, their safety and availability were estimated. Isotopes were rated from one to five, with one being the most favorable and five being the least. Results were then summed to determine scores for each, with a low score being more favorable than a high score. Pu-238 was set as the control, and given the value of three for each category. Categorical improvements on Pu-238 values were rated lower than three. Values that were deemed to be worse than Pu-238 properties were given greater values.

Heat output was rated on specific decay heat for isotopes, with maximum heat values from 107 W/g for Po-210, to 0.117 W/g for Am-241. Decay heat was broken down by order of magnitude of W/g. Greater than 10^1 was given a value of "1", 10^0 was given a value of "2", 10^{-1} was given a value of "3". See table 2.1 for specific decay heats. Exceptions were made for Am-241, Ac-227, and Cs-137. Am-241 was given a point increase as it had the lowest decay heat for all isotopes reviewed. Ac-227 and Cs-137 had low initial values, and then high decay heat values due to daughter products. This resulted in them receiving a point increase as well.

Heat stability was ranked based on the half-life of each isotope. Values on the order of days were given a "5", values in years were given a "4", values in tens of years were given a "3", values in hundreds of years, a "2". No isotopes received a "1" rating.

Safety considerations were based primarily on the magnitude of gamma output in relation to Pu-238. Relative ratings were first given based on Figures 4.8, and 4.9. Magnitudes above Pu-238 were given a "4", Magnitudes below were given a "2". Exceptions were made for Am-241, Cs-137, Cf-252, Cm-244, and Po-210. The Am-241 rating was reduced by a point. While it has a greater rate of gamma decay, it has a lower rate of spontaneous fission than actual Pu-238 fuel. Cs-137 gained a point for the solubility of its chemical form in water. This is a concern for launch safety. Cf-252 and Cm-244 both

gained an additional point due to neutron emissions. Po-210 gained points for toxicity and chemical volatility via sublimation.

Availability was the most subjective measure of an isotopes suitability. Pu-238 is set as the standard for production. Pu-238 is produced via neutron capture by Np-237. Np-238 quickly undergoes beta decay to form Pu-238. Extraction methods are well understood. Through this, it can be seen that there are three major factors in the production of an isotope: source material, irradiation, and extraction. See Section 2.2 for a discussion on production considerations for the selected isotopes.

The required mass of an isotope is linked to its heat output according to chemical form, as shown in Table 4.1, with peak heat values being used for all isotopes. Points are broken down by gram orders of magnitude. Requirements on the order of 10^1 gram are given a value of "1", 10^2 given "2", 10^3 "3", and 10^4 "4". Actinium 227 and Cesium 137 both received unfavorable point increases from their peak decay heat values. This is because their initial values for specific decay heat were much greater, and this increase in heat through decay would lead to additional design issues.

Table 4.2: Ratings of selected isotopes, based on heat output, stability, and estimations of safety, availability, and required mass.

Isotope	Heat Output	Heat Stability	Safety	Availability	Required Mass	Total
Pu-238	3	3	3	3	3	15
Ac-227	2	4	4	4	3	17
Am-241	4	2	3	2	4	15
Cf-252	1	5	5	5	1	17
Cm-244	2	4	5	3	2	16
Cs-137	2	4	4	1	4	15
Po-210	1	5	5	4	1	16
Th-228	1	4	4	5	1	15
Tm-170	1	5	4	4	2	16

With this methodology, Am-241, Cs-137, and Th-228 all emerged as isotopes with potential for use in a deep-space RTG. Cs-137 has real potential for use in radioisotope systems. It is produced in abundance in nuclear reactors, is relatively safe, and has a

high heat output. Its short half-life would preclude it from space missions, as it could not meet long-term power requirements. Th-228 also has potential as a fuel replacement, due to a high heat output, and consequent low mass requirement. Similarly to Cs-137 the Th-228 half-life is too short to provide a reasonable output for space missions. There would be little return on investment for the launch of a Th-228 fueled RTG. Am-241 is selected as the isotope for further review, having the best combination of heat-output, heat-stability, low neutron output and availability. Am-241 has a potentially concerning gamma spectra, with greater energy emission than that of Pu-238, but a neutron output which is several orders of magnitude lower than Pu-238 fuel, which will be analyzed in the next section. Am-241 would require the greatest mass to achieve similar heat outputs of other isotopes reviewed, but also has the greatest potential lifespan of any isotope considered. This would provide a greater initial upfront cost to put an Am-241 fueled RTG in space, but would also potentially provide the greatest return on investment.

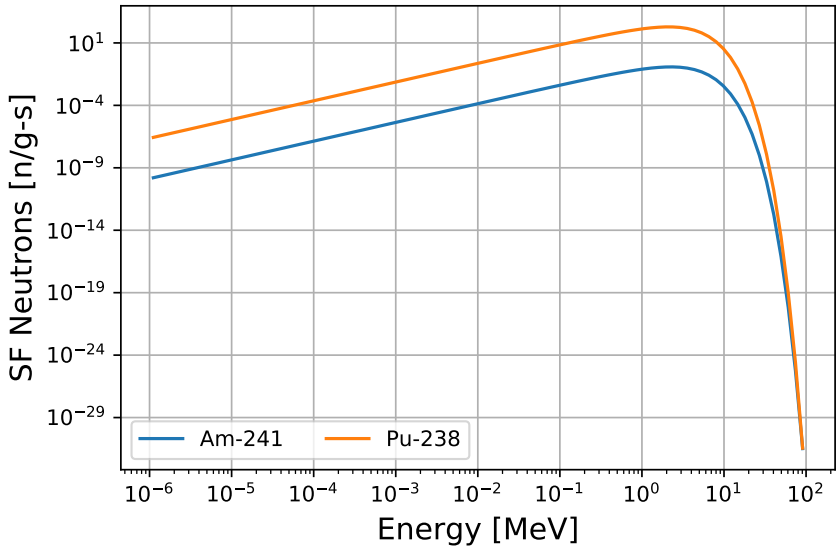

Figure 4.19: Comparison of ORIGEN-generated spontaneous fission neutron spectra for Am-241 and Pu-238 fuel. Pu-238 spectra developed using composition from literature [52].

4.3 MMRTG Radiation Transport Results

4.3.1 Pu-238

A model for a Pu-238 fueled MMRTG was developed for a point of comparison for an Am-241 fueled MMRTG. The developed model and geometry are presented in Figures 3.4, 3.5, 3.6, and 3.7. This model was fully fueled with 32 plutonium pellets clad in DOP-26, each having the same probability of emitting neutrons with the same spectra. The source definition was developed through the isotopic composition presented in [52] and SCALE-ORIGEN. Neutron spectra were generated from SCALE-ORIGEN. Data from the first year of life, including radiation energy bins and probabilities, was exported into a spreadsheet. Any bins with probabilities for emission less than 0.1% were neglected. All remaining bin probabilities were normalized. The remaining bins were each averaged using upper and lower limits to develop a simple mean. The mean energy values were then coupled with their respective source probabilities to generate a quantized version of the spectra generated in SCALE-ORIGEN. This quantized "spectra" was placed in the physics definitions for the radiation source in the MCNP model. Each Pu fuel pellet in the MCNP model was then called in the source definitions so as to allow a neutron to be generated according to the probabilities available from the quantized "spectra" with equal probability anywhere in any of the volumes of the fuel pellets.

Results were generated through mesh tallies. Presented tallies represent voxels defined with multiple steps across x and y axes, and with a single collapsed step in the z axes. Additional tallies were generated, but not presented here to avoid redundancy. Mesh tallies demonstrated n-kev/cm^2 fluence beyond two meters for a fully fueled MMRTG.

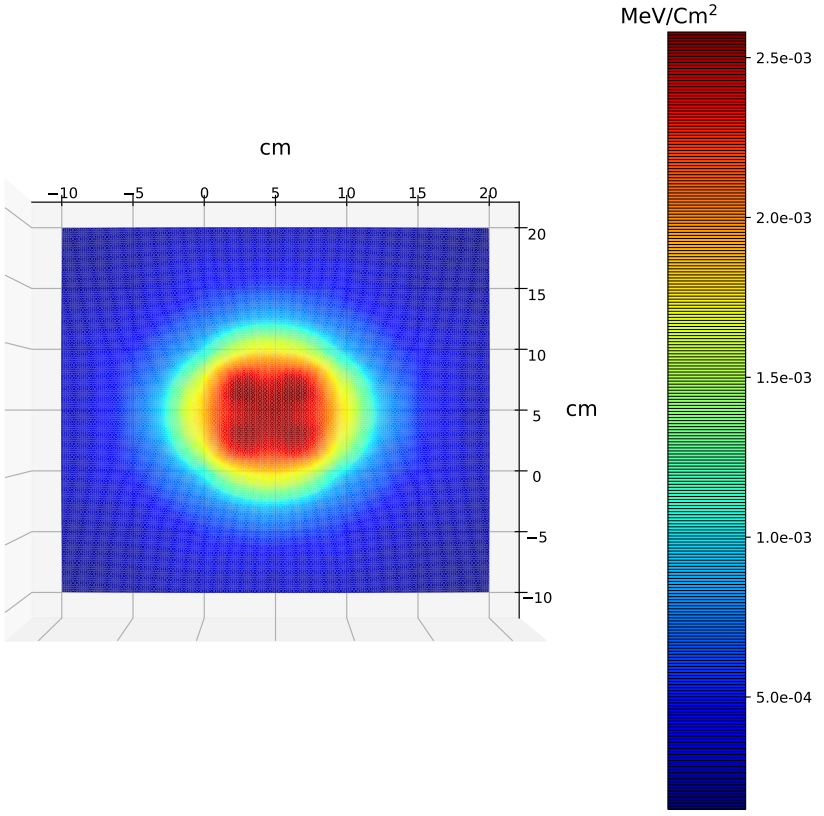

Figure 4.20: Contour plot of MMRTG neutron transport mesh tally with results in MeV/cm^2 per source neutron. Boundaries account for the diameter of the MMRTG exterior cylinder, with the origin (0,0) being one corner of the first GPHS unit in the eight unit stack.

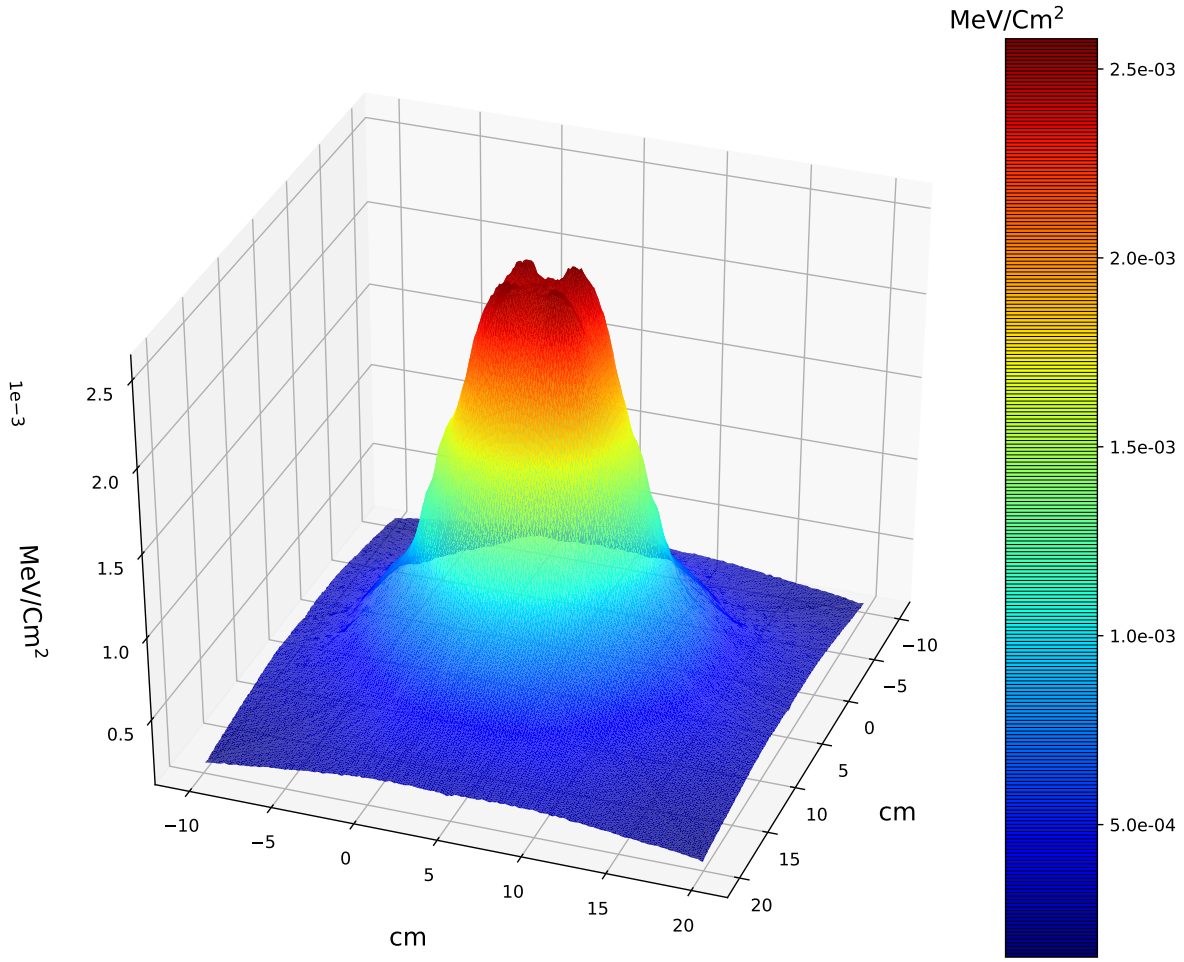

Figure 4.21: Surface plot of MMRTG neutron transport mesh tally with results in MeV/cm^2 per source neutron. Boundaries account for the diameter of the MMRTG exterior cylinder, with the origin (0,0,0) being one corner of the first GPHS unit in the eight unit stack.

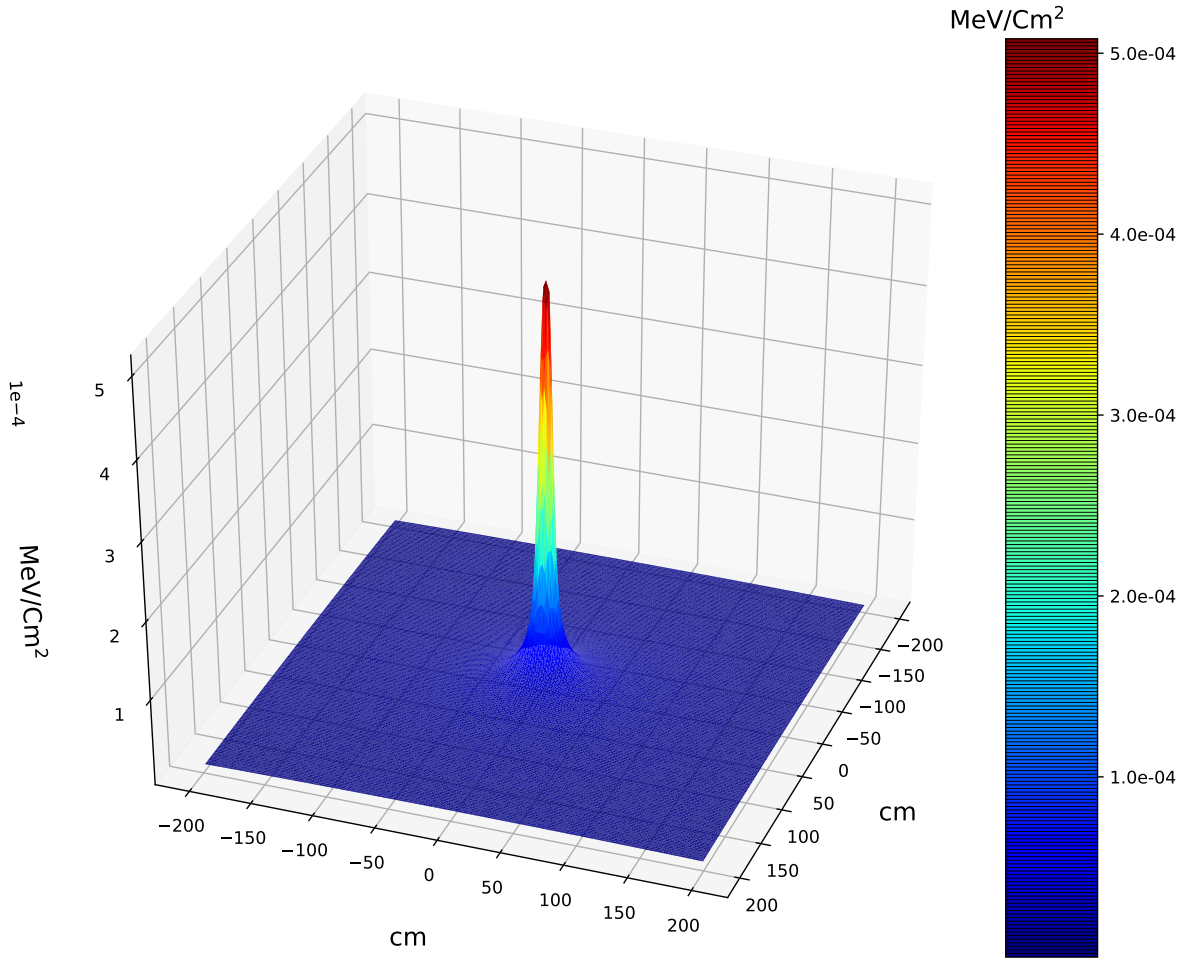

Figure 4.22: Surface plot of MMRTG neutron transport mesh tally with results in MeV/cm^2 per source neutron. Boundaries are extended to +/- two meters from the center of the MMRTG model with the MMRTG model in air.

4.3.2 Am-241

To develop an Americium fuel source for an MMRTG, the first consideration was the thermal requirement, and requisite mass. The required mass and volume to meet the 2000 thermal watt heat requirement, assuming pure Am-241, was given in Table 4.1. A cylindrical source was developed for uniform heat distribution. Using the dimensions for a stack of eight GPHS units, a maximum height and radius were found. Using these values, a height and radius for an Am-241 fuel cylinder were found such that the minimum radial wall thickness was the same as the vertical wall thickness, with a total volume of 1,648 cm^3 of Am-241 fuel. All GPHS units were removed from the Pu fueled

MMRTG, and were swapped with a carbon rectangular cuboid of the same material used to model the GPHS aeroshell, with the same dimensions as eight stacked GPHS units. The interior of this contained the Am-241 oxide fuel cylinder, with a DOP-26 cladding of the same thickness specified for plutonium fuel.

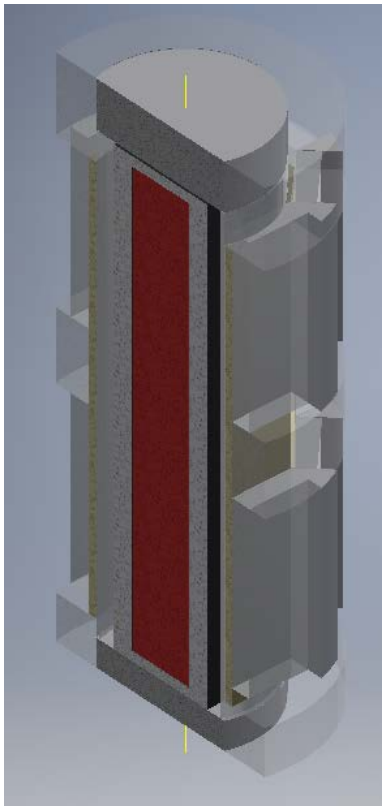

Figure 4.23: CAD rendering of Am-241 fueled MMRTG. Exterior containment is neglected in CAD model but is utilized in MCNP model.

Due to the relatively low spontaneous fission rate of Am-241 (see Figure 4.19) neutron production and transport was neglected for the Am-241 fueled RTG. Gamma spectra were generated through SCALE-ORIGEN in a manner similar to the development of neutron spectra for the Pu model. Am-241 gamma spectra can be seen in Figure 4.17. An isotopically pure oxide sample was assumed, as such the data for the first year of fuel life was used to develop a gamma source for MCNP, which was applied to an Am-241 fueled model.

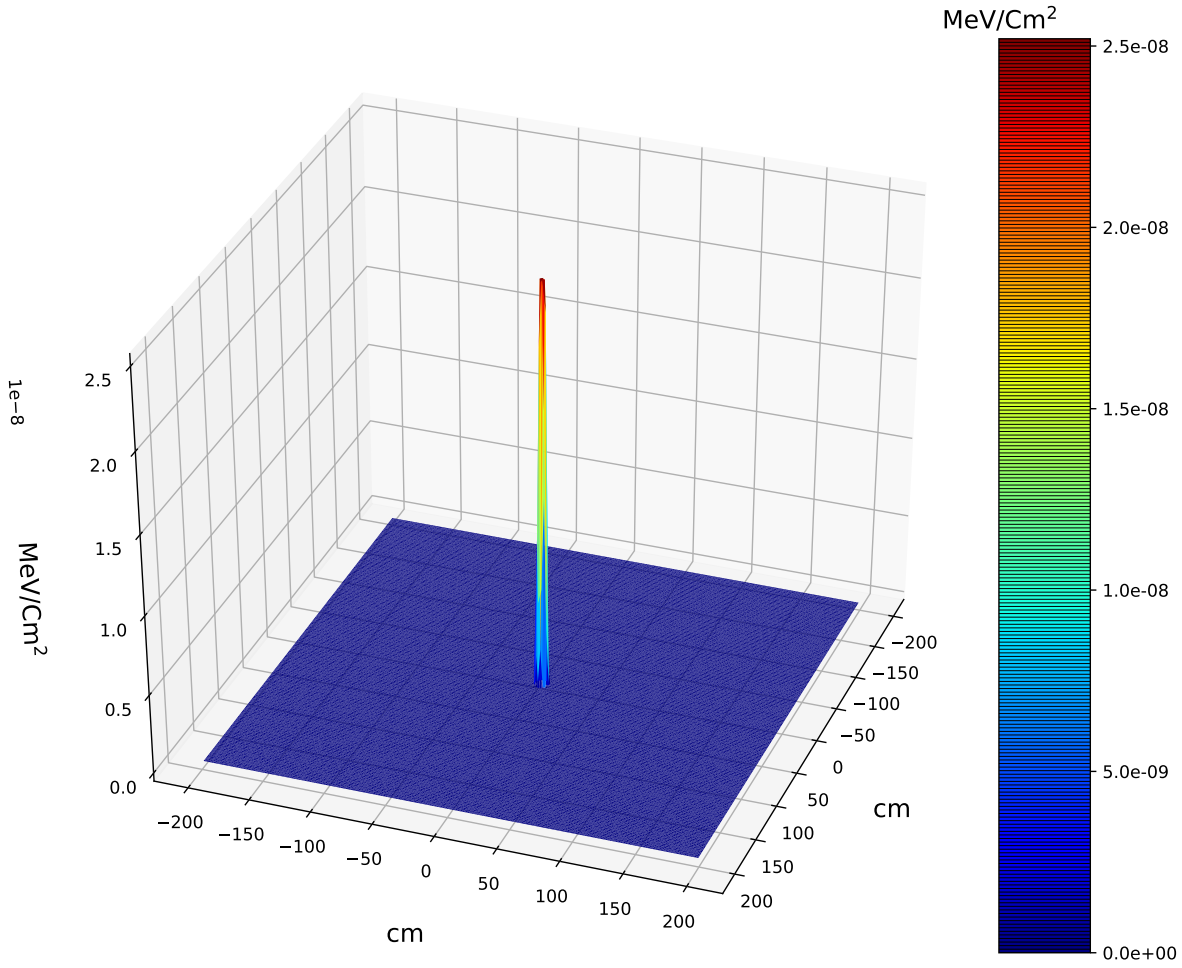

Figure 4.24: Surface plot of Am-fueled MMRTG photon transport mesh tally with results in MeV/cm^2.

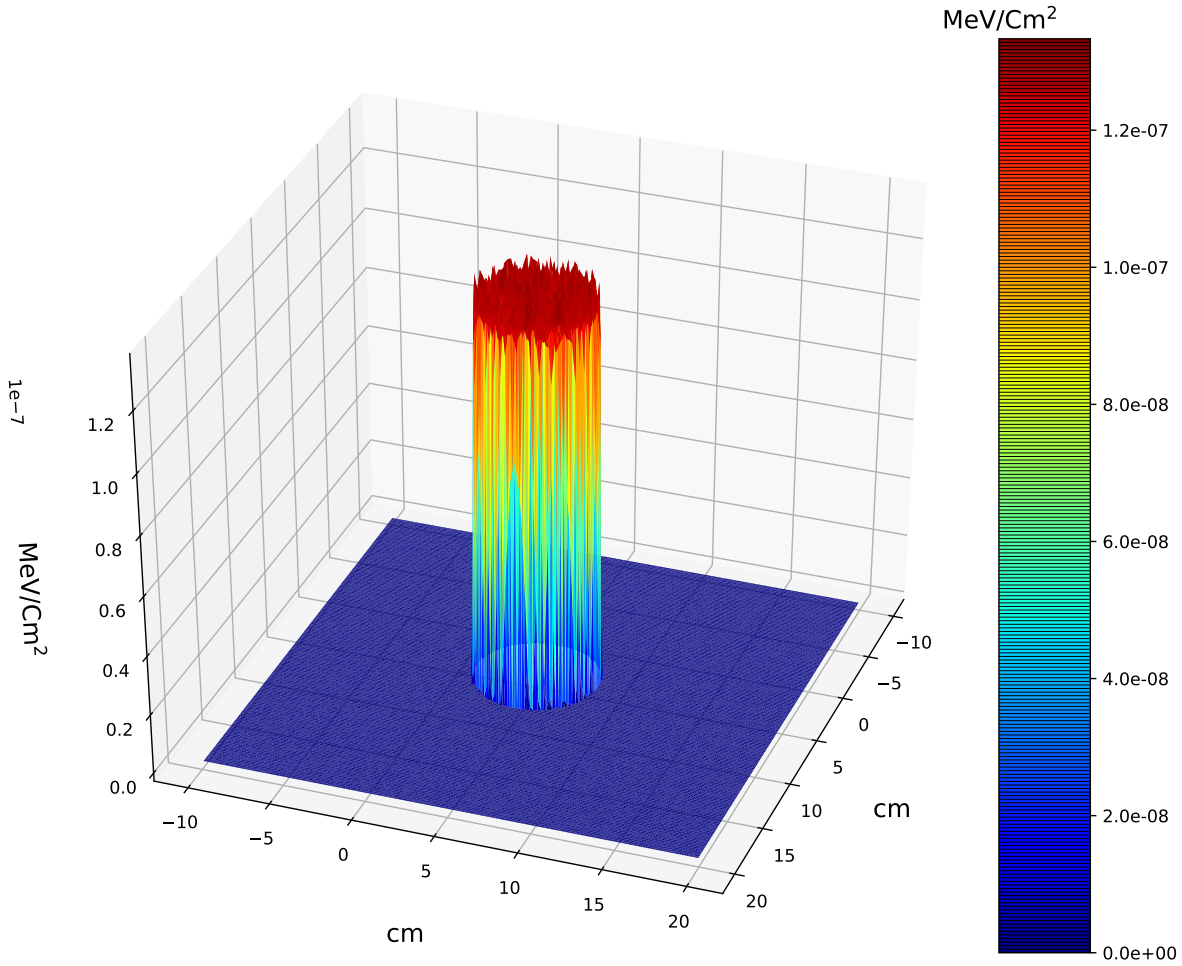

Figure 4.25: Surface plot of Am-fueled MMRTG photon transport mesh tally with results in MeV/cm^2.

Initial results for the gamma source indicate that the DOP-26 clad was an effective shield for the Am-241 gamma spectra. While it appears that all gammas dropped off at the edge of the fuel cylinder, this is not the case. MCNP6 calculated energy levels below the cutoff (about 1eV) such that it was not necessary to continue tracking photons.

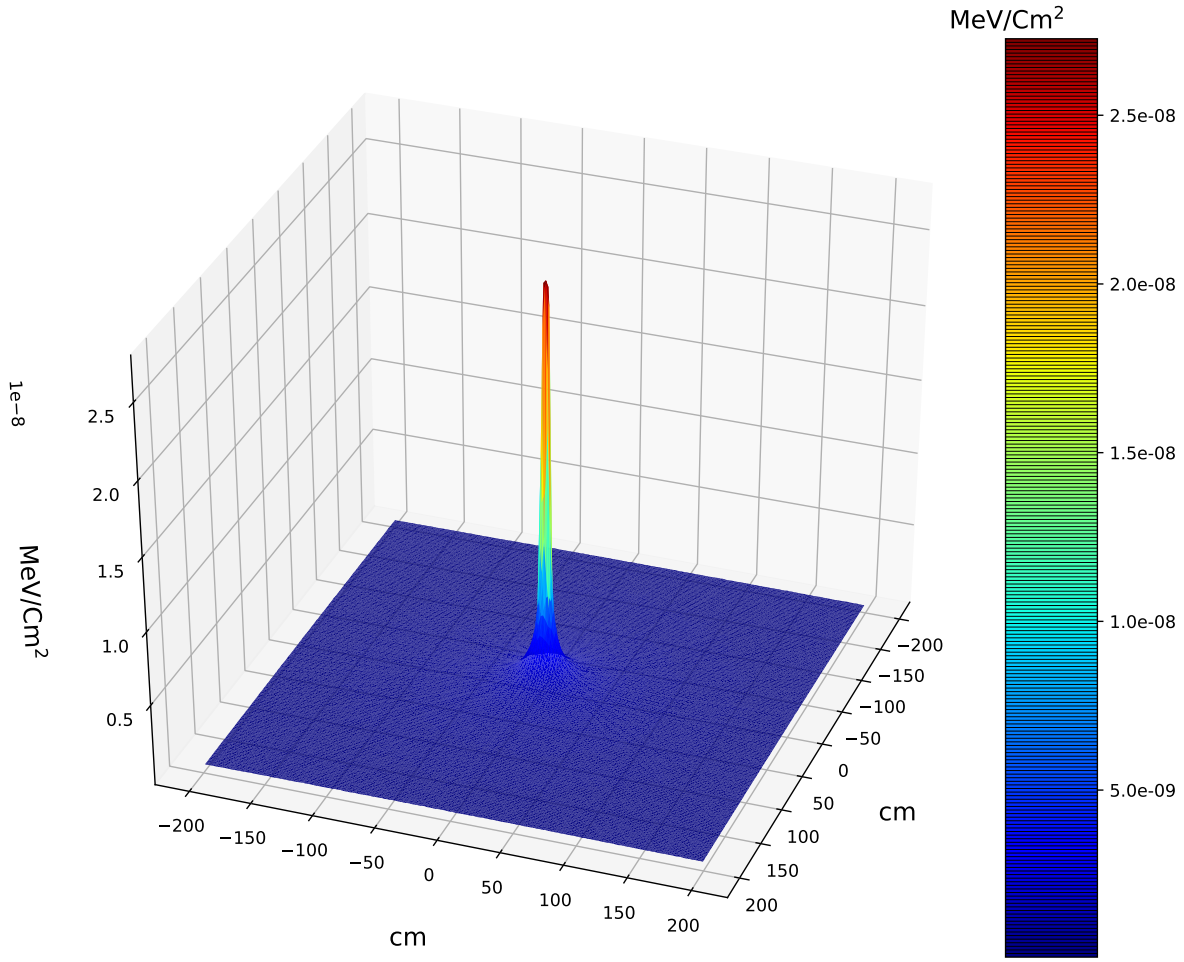

Figure 4.26: Surface plot of Am-fuel bare cylinder photon transport mesh tally with results in MeV/cm^2. Results are shown for a four meter square grid, with the MMRTG centered.

As an added check, the same physics were used to model a bare cylinder in air. This demonstrated that a bare cylinder of the amount of Am-241 necessary for 2000 W thermal output, had a lower flux than an MMRTG fully fueled with plutonium (see figure 4.22), with radiation more easily shielded than the neutrons produced via spontaneous fission in plutonium fuel.

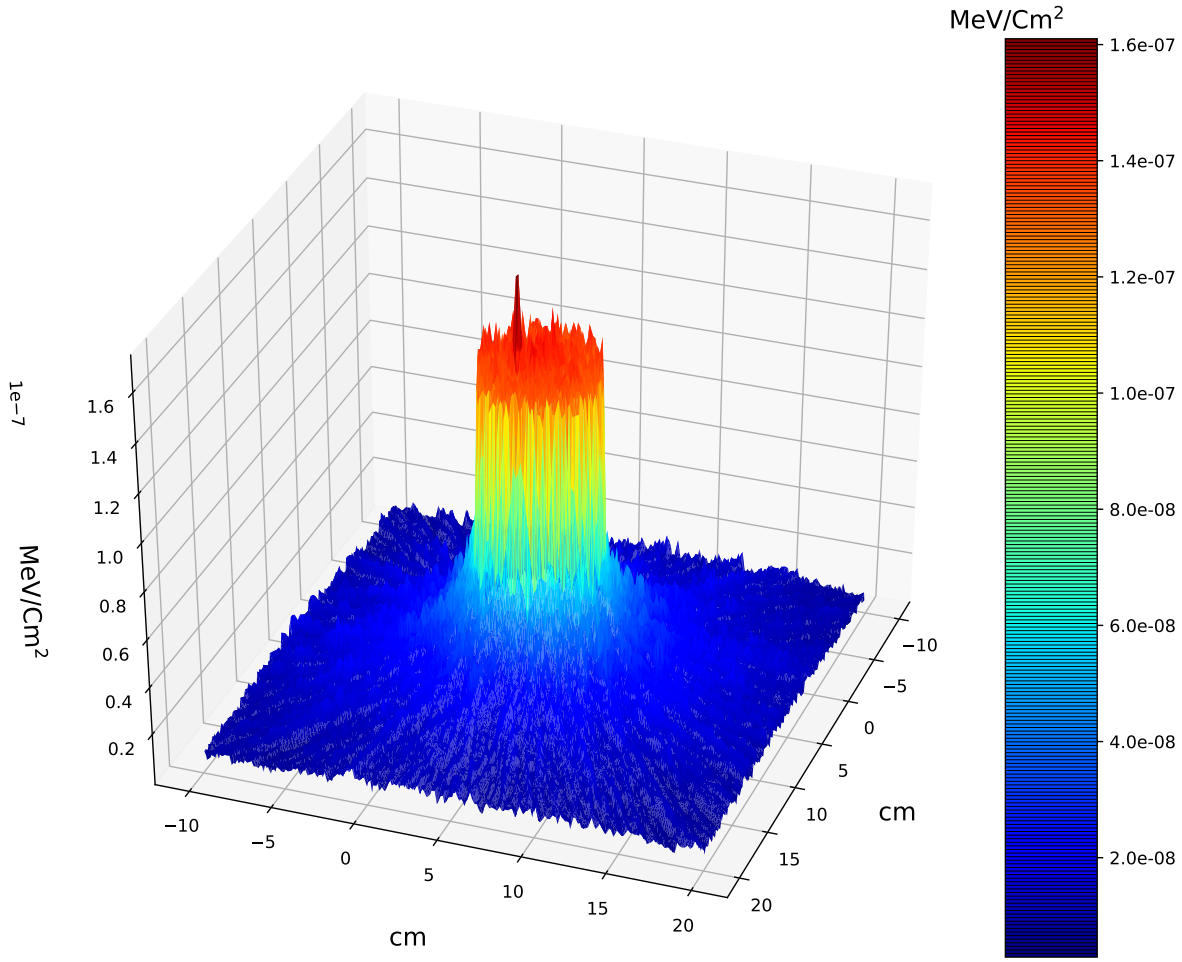

Figure 4.27: Surface plot of Am-fuel bare cylinder photon transport mesh tally with results in MeV/cm^2. Results are shown in a 30 by 30 cm grid.

4.3.3 Thermocouple Comparison

An assumption was made in the development of an MMRTG MCNP model that TCs modeled with homogeneous materials would behave similarly to TCs modeled with heterogeneous material. Meaning that in the model developed, the PN thermocouple materials, PbTe, PbSnTe, and TAGS (see Figure 2.1) were homogenized such that all volumes contained the same composition.

The homogenization was done using best engineering judgment to account for the volume of each material in each cold shoe, see Figure 2.1. This information fed into the determination of mass for each material, using an estimated density, as densities of

the crystals were unavailable. Total mass was then coupled with total volume, and a homogeneous material density was determined using a weighted average for the density of each material. MCNP material compositions were then normalized so as to develop a weighted, multi-atom, single-material input card.

For example, the most simple case is the PbTe material, which has an approximately equal molecular composition, with an atomic ratio of 1 (1 part Pb to 1 part Te). Lead has a molecular weight (MW) of about 207.2 AMU, and Tellurium has an MW of about 127.6 AMU. The density of pure Pb is approximately 11.34 g/cc, and 6.24 g/cc for Te. Using these values, the molar density for each component can be found. Using an equal weighting, the average molar density of the material is found. The molar density and atomic ratio feed into the determination of a molar volume fraction. This value is multiplied by the estimated volume fraction of the PbTe material in the P-N thermocouple. This gives a volume fraction for each species in the TC. Using the density of the pure material again, a mass basis is found. This feeds into a mass fraction, and an average density for the material. The average densities for the material are weighted by the volume fractions of each material to determine an average density for the entire TC. The molar density for the materials are used with the atomic ratios to find molar fractions of each species in each material. These values are then divided by the total molar fractions to find the atomic fractions of each species. Lead and Tellurium appear multiple times, and as such, their fractions were combined. All of these fractions were then fed into a single MCNP material card. For nonhomogeneous TC models, each material (PbTe, TAGS, PbSnTe) had its own material cards, with densities estimated in a similar manner. Physics for this problem were copied directly from the Pu-238 MCNP input file.

To test whether this assumption and methodology was valid, two models were developed. Variation between homogeneous and heterogeneous material were observed.

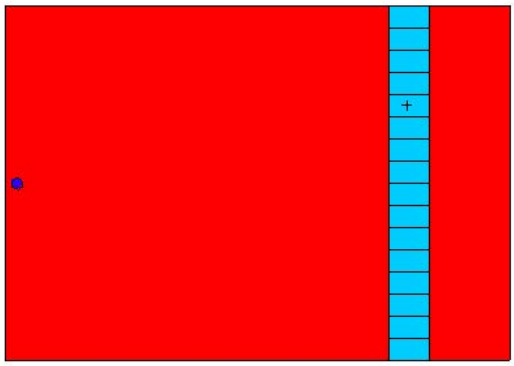

Figure 4.28: Vised rendering of general TC homogeneous vs. heterogeneous model. Side view. Red indicates air, dark blue is the Pu source, light blue is the TC array. See Figure 3.5 for homogeneous arrangement of TC's.

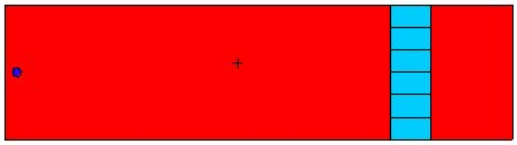

Figure 4.29: Vised rendering of general TC homogeneous vs. heterogeneous model. Top view. Red indicates air, dark blue is the Pu source, light blue is the TC array. See Figure 3.5 for homogeneous arrangement of TC's.

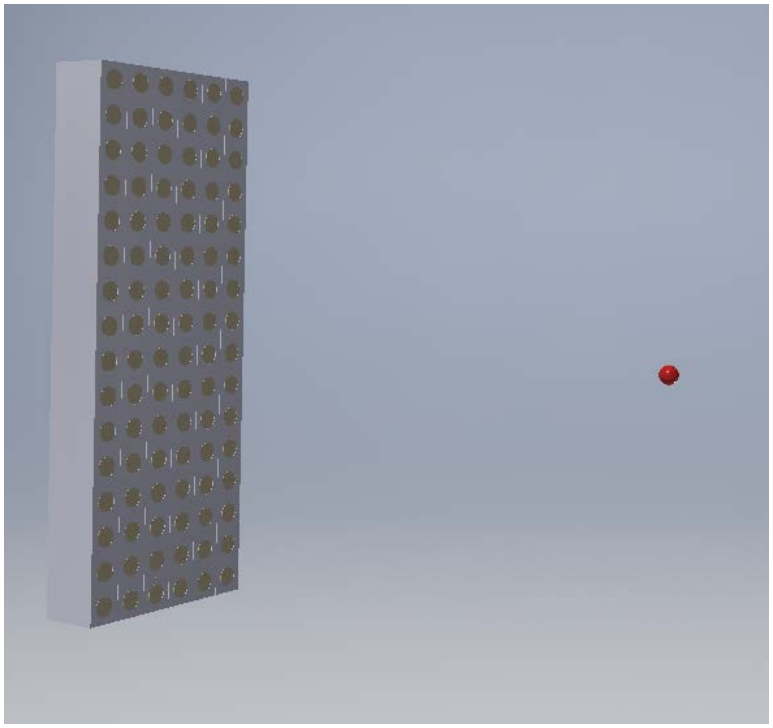

Figure 4.30: CAD rendering of homogeneous TC model.

Each thermocouple array for this model was the same size and configuration as one theromocouple array modeled in the full MMRTG model, see figure 3.5. Each of these was exposed to a 0.5 cm diameter spherical isotropic plutonium source with approximately the same composition of Pu isotopes found in MMRTG fuel, centered 17 cm from the array. The atmosphere for these models was air. An approximate neutron spectrum for this source was generated in SCALE-ORIGEN using the isotopic composition of Pu fuel. This was the same spectrum used in the Pu-238 fueled MMRTG MCNP model. Probabilities and energy levels were normalized from ORIGEN for the MCNP source definition.

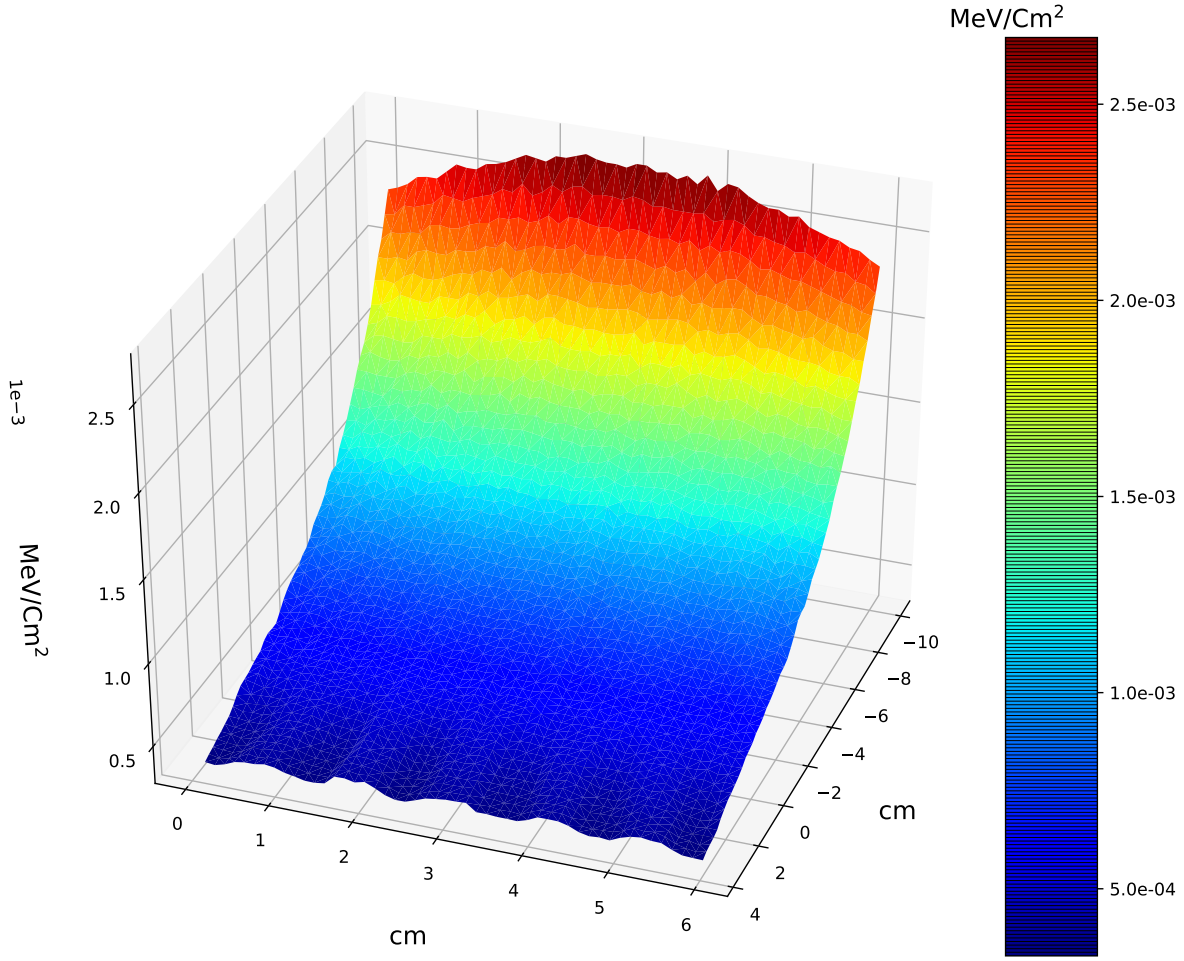

Figure 4.31: Energy flux averaged over cells for homogeneous TC material. Source material is outside the boundary of visualization.

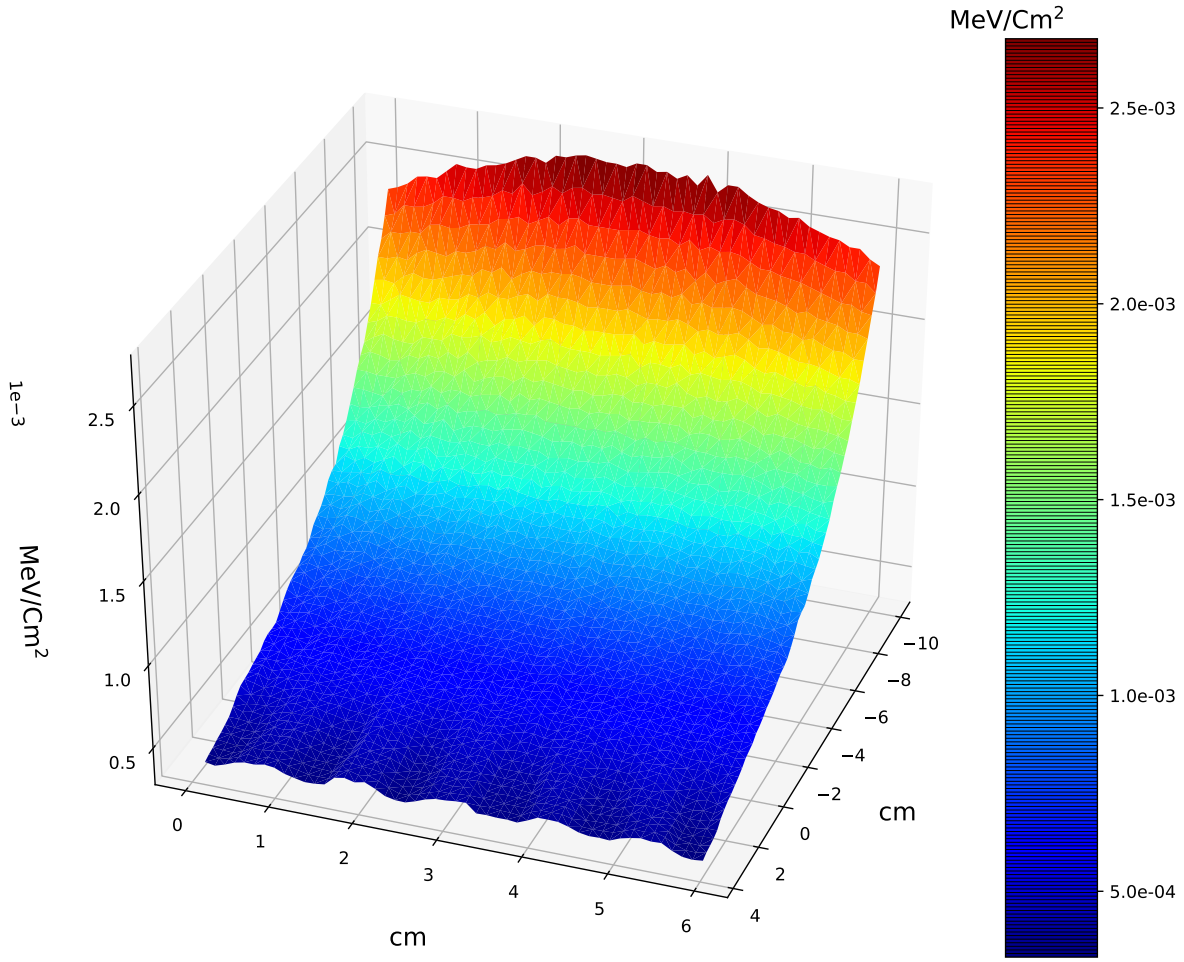

Figure 4.32: Energy flux averaged over cells for heterogeneous TC material. Source material is outside the boundary of visualization.

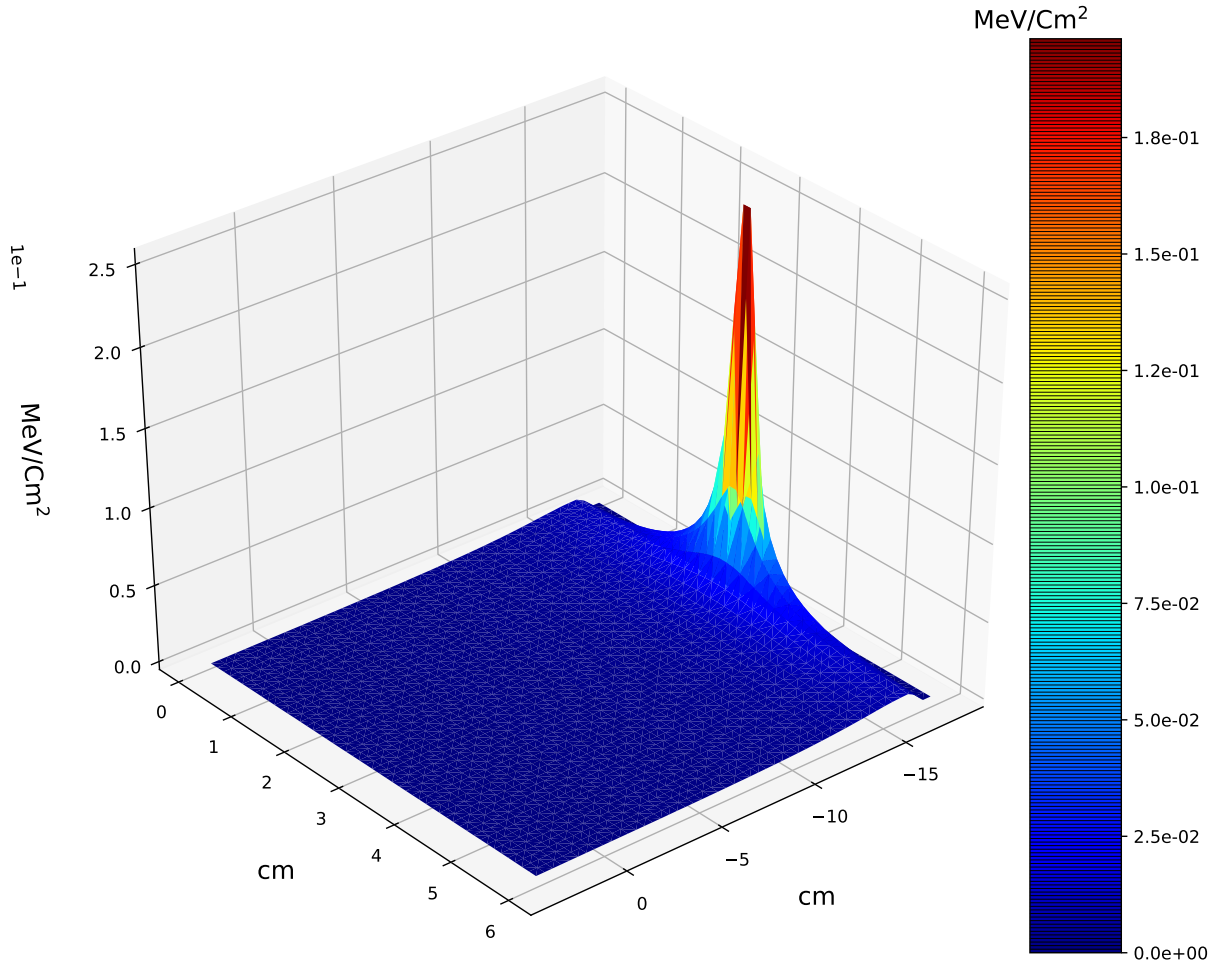

Figure 4.33: Energy flux averaged over cells for homogeneous TC material. Peak is due to isotropic source material. Zero values indicate an area of zero importance (IMP:n=0) as defined in model.

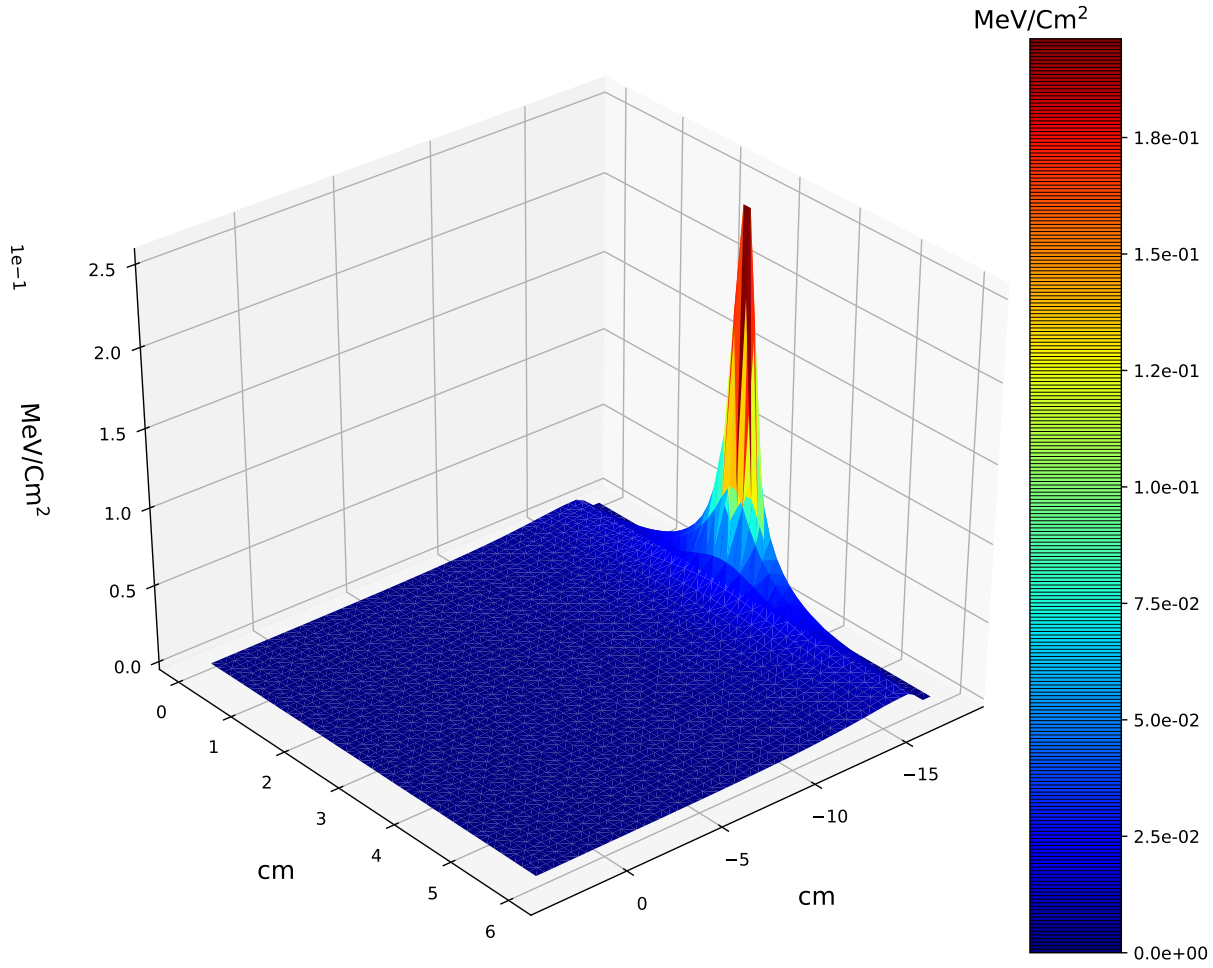

Figure 4.34: Energy flux averaged over cells for heterogeneous TC material. Peak is due to isotropic source material. Zero values indicate an area of zero importance (IMP:n=0) as defined in model.

Results demonstrated neutron flux, in MeV/cm^2 with less than a percent difference between models. This provides evidence for the validity of the TC material homogenization approximation.

Chapter 5

Discussion

5.1 Results

5.1.1 Limitations of Current Work

Due to the nature of the MMRTG, and its export controlled status, finding accurate material properties proved difficult. As this work proceeds into the future, more accurate material compositions will be sought to place within the models, as well as more accurate dimensions. There was great confidence in the geometry of the GPHS units within the model, as this information is readily available in literature. The MMRTG geometry has been much more difficult to obtain. Best engineering judgment was used to develop the MMRTG, though there is much uncertainty. Fortunately, MCNP makes redefining geometry quite straightforward. As more accurate dimensions become available, these can be readily applied to improve the models that were developed.

In this study, gamma output between radioisotopes was compared directly, on a gram basis. This basis was chosen to provide a valid point of comparison, but this only provides one facet for comparison. Additional work will be done with normalized values for the relative required mass of material to produce the same heat output. This will provide information on the relative radiation output. This would likely have a small effect on the radiation output calculated, as differences in output (MeV/g-s) were generally several orders of magnitude apart, while mass requirements would likely be within an order of magnitude. This scaling will be beneficial for a point of reference in future work, but is not necessary for this study.

Tallies presented are 2-D representations of 3-D problems. Flux was not radial, but sources were isotropic, and all emission probabilities were normalized using the same

method. The mesh tallies generated functionally compress flux over a volume into a surface by having multiple delimiters in the x and y directions, but only one in the z direction. Due to the nature of MCNP tallies, the same model could have very different results depending on how the tally is defined. This is why, in this study, models to be compared were all given the same mesh tally code. This was done to maintain consistency between flux results. The comparison of relative magnitudes for radiation transport is valid as all models were developed with the same basic geometries, with mesh tallies representing the same volumes, and results between models being comparable.

5.1.2 Preliminary Performance of Am-241

Am-241 is a viable fuel source for radioisotope thermoelectric generation, having lower outputs of easily shielded gamma radiation than a Pu fueled RTG, and its spontaneous fission neutrons. In terms of radiation safety, Am-241 is a superior fuel source. Other considerations are needed with the additional 11 kg of Am-241 fuel required versus Pu fuel to achieve the same 2000 Watt thermal output. Some advantage may be gained on the front-end of fuel fabrication from the relatively low radiation output, with next to zero spontaneous fission neutrons. This coupled with the long half life means that an Am-241 fueled RTG may have the potential for a longer design life in space missions than a Pu-238 fueled RTG.

5.2 Future Work

The melting point of various potential fuel forms is a very important factor in the selection of radioisotopes for heat generation. While this was considered to be outside the scope of this study, all forms chosen for this study should be physically stable. Future work should more thoroughly review fuel in terms of various forms, densities, and melting points. Additionally, work could consider the effects that transmutation would have on fuel forms and geometry over time. For this study, only one fuel form

per isotope was considered. This would be of particular interest for Am-241, as it has several potential oxidation states, and a review of their potential impact on fuel integrity and longevity would be an important consideration for future design efforts. It was not necessary to perform an exhaustive review of all chemical forms available for this study, only to provide information for feasible fuel forms for each radioisotope.

There are a number of radioisotopes which have a greater heat output than Am-241, but were not reviewed in this work. Am-241 was ultimately chosen as the alternative fuel source for review because of its relative safety and availability. Am-241 has the lowest heat rate relative to the other isotopes reviewed in this work. Consequently, the consideration of additional fuel sources with greater heat output likely would not change the results of the selection. There is a possibility that the addition of other radioisotopes could impact selection through additional work, but the data generated from this study points to this being unlikely. Potential isotopes had already been down selected, as covered in Chapter 1, Section 1.

Certain isotopes that have been viewed as potentially viable for RTG applications in the past, such as Sr-90, were not considered in this work. Broadening the field could have an impact on the selection of isotopes for further review. This could be a valuable output of future work.

Pu-236 is unavoidable in the production of Pu-238. Pu-236 has a 2.86 year half-life, and a decay-chain with numerous problematic gamma emitters. Chemical separation techniques would be unable to differentiate between Pu-236 and Pu-238. One way to manage Pu-236 would be to allow the Pu-238 source material to decay and thereby increase the potential for a more pure fuel. Unfortunately, the half-life of Pu-238 is such that as the Pu-236 decayed, so too would the Pu-238. Additionally, the decay products of the Pu-236 further exacerbate issues with safety and chemical processing. In counterpoint, Am-241 is produced from decay products of used nuclear fuel, and exists as a highly pure isotope. After chemical separation, the remaining americium would be a high-purity Am-241 due to the general lack of other forms of americium in

the fuel source. Am-241 fuel can be produced as a more isotopically pure, and thereby potentially safer fuel than Pu-238. Future work will do a direct comparison of gamma outputs for Am-241 and Pu-238 fuel with added focus on isotopic impurities in both of these.

5.2.1 Current Model

Additional work should be completed to convert radiation transport results into a more meaningful representation such as a dose rate. This would allow results to be presented more generally. Flux is a useful measure of the radiation transport between models. Dose rate would provide knowledge required to inform shielding requirements to enhance the safety of operations for the alternatively fueled RTG.

The current models may be used to provide information on the behavior of an Am-241 fueled MMRTG in different environments, similar to the work done at ORNL [52]. As a fully Pu-238 fueled Pu-238 model was developed in conjunction with the Am-241 model, this could also be used in future work. Additional work could be performed with the current models to determine radiation transport behavior over time. Outputs generated from this work already have radiation profiles for fuel sources over time. These outputs include gamma and neutron spectra, as well as transmuted isotopes and concentrations. This data can be readily used to develop additional physics inputs for future MCNP models.

5.2.2 Model Enhancement

The fuel geometry for Am-241 utilized in these models is convenient, but may be unrealistic. To use Am-241 with the same power requirements, numerous changes to the MMRTG would need to be made. The fuel form, as presented in this work would be difficult to fabricate. The GPHS stacks, which provide containment in the event of a mission failure, would need to be replaced with another containment system. And likely, an alternate TC array would need to be developed to capitalize on the new heat delta

that would occur with a new fuel configuration. This is an important consideration for any new fuel type, as having the theoretical heat output needed is only one piece of the puzzle for developing a new fuel source. Its mass and volume would necessitate specialized equipment to manufacture, including mills, lathes, furnaces, glove-boxes, etc. as well as new procedures and specialized equipment for transportation. This would feed into a cost analysis. As the ESA has done, it may be beneficial for future modeling and design work to focus on RTGs with lower power requirements, and compatible fuel geometries.

References

[1] World Nuclear Association. *Nuclear Reactors and Radiosotopes for Space*. World Nuclear Association (2018).
http://www.world-nuclear.org/information-library/non-power-nuclear-applications/transport/nuclear-reactors-for-space.aspx

[2] NASA. *Radioisotope Power Systems: The Power to Explore*. NASA (2015).
https://rps.nasa.gov/system/downloadable_items/29_APP_RPS_Prog_FS_2015_1-13-151.pdf

[3] K. Northon, *NASA's Three-Billion-Mile Journey to Pluto Reaches Historic Encounter*. NASA (2015).
https://www.nasa.gov/press-release/nasas-three-billion-mile-journey-to-pluto-reaches-historic-encounter

[4] D. Mosher, *NASA's Plutonium Problem Could End Deep-Space Exploration*. Wired (2013).
https://www.wired.com/2013/09/plutonium-238-problem/

[5] R. Walli, *ORNL Achieves Milestone With Plutonium-238 Sample*. Oakridge National Laboratoy (2015)
https://www.ornl.gov/news/ornl-achieves-milestone-plutonium-238-sample

[6] L. Summerer, and K. Stephenson, *Nuclear Power Sources: A Key Enabling Technology for Planetary Exploration*. Proceedings of the Institution of Mechanical Engineers, Part G: Journal of Aerospace Engineering **225** (2011) 129–143.

[7] I. Hore-Lacy, *Can Americium Replace Plutonium in Space Missions?*. World Nuclear News (2014).

http://www.world-nuclear-news.org/Articles/Can-americium-replace-plutonium-in-space-missions

[8] Los Alamos National Lab, *MCNP User's Manual, Version 6.0*.

[9] A. Romero-Wolf, Et. Al., *Prospects of passive radio detection of a subsurface ocean on Europa with a lander*. Planetary and Space Science **129** (2016) 118–121.

[10] A. Masters, Et. Al., *Neptune and Triton: Essential pieces of the Solar System puzzle*. Planetary and Space Science **104** (2014) 108–121.

[11] J. Moore, Et. Al., *The Geology of Pluto and Charon Through the Eyes of New Horizons*. Science **351** (2016) 1284–1293.

[12] C. Gebhardt, *New Horizons prepares for New Year's Day 2019 Kuiper Belt Object encounter*. NASA Spaceflight (2017). https://www.nasaspaceflight.com/2017/01/new-horizons-2019-kuiper-belt-encounter/

[13] R. Mulford, *Radioisotopic Thermoelectric Generator (RTG) Surveillance*. Los Alamos National Lab Technical Report (2016).

[14] D. Vondy, J. Lane, and A. Gresky, *Production of Np237 and Pu238 in thermal power reactors*. Industrial & Engineering Chemistry Process Design and Development **3** (1964) 293–296.

[15] R. O'Brien, Et. Al., *Safe Radioisotope Thermoelectric Generators and Heat Sources for Space Applications*. Journal of Nuclear Materials **377** (2008) 506–521.

[16] G. Robertson, Et. Al., *Preliminary Analysis: Am-241 RHU/TEG Electric Power Source for Nanosatellites*. Nuclear and Emerging Technologies for Space (2014).

[17] T. Tinsley, *Can Nuclear Waste Help Humanity Reach for the Stars?*. The Planetary Society (2015).

http://www.planetary.org/blogs/guest-blogs/2015/0423-can-a-nuclear-waste-help-humanity-reach-for-the-stars.html

[18] ESA, *Rosetta's Last Words*. European Space Agency (2016). http://www.esa.int/Our_Activities/Space_Science/Rosetta/Rosetta_s_last_words_science_descending_to_a_comet

[19] R. Ambrosi, Et. Al., *Americium-241 Radioisotope Thermoelectric Generator Development for Space Applications*. International Nuclear Atlantic Conference (2013).

[20] W. R. Corliss, R. L. Mead. *Power from Radioisotopes.* United States Atomic Energy Commission (1963) 1-6.

[21] G. H. Rinehart *Design Characteristics and Fabrication of Radioisotope Heat Sources for Space Missions.* Progress in Nuclear Energy **39(3-4)** (2001) 305–319.

[22] W. R. Corliss, R. L. Mead. *Power from Radioisotopes.* United States Atomic Energy Commission (1963) 35.

[23] W. R. Corliss, R. L. Mead. *Power from Radioisotopes.* United States Atomic Energy Commission (1963) 39.

[24] D. Harris, J. Epstein. *Properties of Selected Radioisotopes.* National Aeronautics and Space Administration (1968) 3.

[25] G. M. Fradkin, V. M. Kodyukov. *Radioisotope Thermoelectric generators.* Translated from: Atomnaya Énergiya **26(2)** (1969) 169–175.

[26] G. Bennett, *Space Nuclear Power: Opening the Final Frontier.* International Energy Conversion Engineering Conference and Exhibit (IECEC) (2006).

[27] G. R. Schmidt, M. G. Houts. *Radioisotope based Nuclear Power Strategy for Exploration Systems Development*. AIP Conference Proceedings (2006).

[28] H. R. Williams, et. al. *A Conceptual Spacecraft Radioisotope Thermoelectric and Heating Unit (RTHU).* International Journal of Energy Research **36** (2012) 1192–1200.

[29] V. V. Gusev, et. al. *Milliwatt-Power Radioisotope Thermoelectric Generator (RTG) Based on Plutonium-238.* Journal of Electronic Materials **40(5)** (2011) 807–811.

[30] W. A. Wong *Advanced Radioisotope Power Conversion Technology Research and Development*. International Energy Conversion Engineering Conference (2004).

[31] D. J. Anderson, W. A. Wong, K. L. Tuttle. *An Overview and Status of NASA's Radioisotope Power Conversion Technology NRA*. International Energy Conversion Engineering Conference (2005).

[32] D. Woerner, *A Progress Report on the EMMRTG*. Journal of Electronic Materials **45(3)** (2016) 1278–1283.

[33] C. Groupen. *Introduction to Radiation Protection.* Springer Verlag, Berlin Heielberg (2010) 323-325.

[34] T. Tinsley, Account Director at National Nuclear Laboratory, UK. Personal Communication (2018).

[35] R. A. Schwarz, S. F. Kessler, T.A. Tomaszewski. *Dose Rate Visualization of Radioisotope Thermoelectric Generators*. Space Technology and Applications International Forum (1996).

[36] T. Seebeck, *Magnetische Polarisation der Metalle und Erze Durch Temperaturdifferenz*. W. Engelmann (1895).

[37] Caltech, *Brief History of Thermoelectrics*. Caltech Materials Science (2018). `http://www.thermoelectrics.caltech.edu/thermoelectrics/history.html#top`

[38] NASA. *Multi-Mission Radioisotope Thermoelectric Generator (MMRTG) NASA (2013).*
https://mars.nasa.gov/mars2020/files/mep/MMRTG_FactSheet_update_10-2-13.pdf

[39] I. Jun, S. Kang, R. Evans, M. Cherng. *Radiation Transport Tools for Space Applications: A Review.* Geant4 Space Users' Workshop (2008).

[40] R. Cataldo, G. Bennett. *US Space Radioisotope Power Systems and Applications: Past, Present and Future* Radioisotopes-Applications in Physical Sciences (2011).

[41] NASA, *Thermal Systems: General Purpose Heat Source.*
https://rps.nasa.gov/power-and-thermal-systems/thermal-systems/general-purpose-heat-source/

[42] A Schock, A. Shostak, H. Sookiazian, *Design, Analysis, and Optimization of RTG for Solar Polar Mission.* Intersociety Energy Conversion Engineering Conference (1994)

[43] A Schock, C. Or, *Effect of Fuel and Design Options on RTG Performnace Versus PFF Power Demand.* Intersociety Energy Conversion Engineering Conference (1994).

[44] Visual Editor Consultants *MCNPX Visual Plotter v 2.7.E (2011).*

[45] G. Bennett, Et. Al., *Mission of Daring: the General-Purpose Heat Source Radioisotope Thermoelectric Generator..* International Energy Conversion Engineering Conference and Exhibit (IECEC) (2006).

[46] Haynes International *Haynes 25 Alloy Product Sheet (2017).*

[47] J. Hemrick, E. Lara-Curzio, J. King, *Characterization of min-k te-1400 Thermal Insulation.* ORNL Technical Report, ORNL (2008).

[48] Microtherm *Product Performance Brochure (2018).*

[49] R. Taylor, H. Groot, *Thermophysical Properties of POCO Graphite.* Purdue University Lafeyette Ind Properties Research Lab (1978).

[50] D. Pierce, et. al., *Grain Growth and Precipitation Behavior of Iridium Alloy DOP-26 During Long Term Aging.* ORNL Technical Report, ORNL (2017).

[51] Pacific Northwest National Laboratory Isotope Program, *Actinium 227.* `https://radioisotopes.pnnl.gov/isotopes/thorium-227.stm`

[52] M. B. R. Smith. *Radioisotope power source dose estimation tool (RPS-DET).* IEEE Aerospace Conference (2018).

Appendix A: SCALE-ORIGEN Example Input

```
=origen
bounds{
   gamma=[240i  1E4 1.0E-7] %241 linear bins
   neutron=[90L 1e8 1] %91 log bins
}
case(Am-241){
   gamma=yes
   neutron=yes
   lib{ file=end7dec }
   time{
       t=[240i 0.0 30] % Linear steps = i, 30 years
       units=years
   }
   mat{
     iso=[Am241=1] %
     units=GRAMS %units in iso array
   }
   print{
      nuc{ total=yes units=[GRAMS WATTS] }
      gamma{ spectra=yes
             summary=yes
      }
      neutron{
            summary=yes
            spectra=yes
```

```
      }
   }
'   gamma{
'     sublib=ALL    % ALL = all sub-libraries
'                   %
'     continuum=yes % expand continuum data stored as
'                   % lines into proper continuua
'     immediate=yes % load lines for immediate gamma/x-rays
'     spont=yes     % include photons from spont fiss
'    }
    save{ steps=all }
    % save all information to f71
    %
}
end
```

Appendix B: Example of Surface Plotting in Python, Using MCNP FMesh Tally

```
import os
import pandas as pd
import matplotlib.pyplot as plt
from matplotlib import cm

os.chdir("C:/Users/nwill/Desktop/MMRTG/Data_work")
#enter correct directory

df = pd.read_csv('Pu_tc_hetero_meshtal_1.csv', parse_dates=True)
fig = plt.figure(figsize=(10,8))
ax = fig.add_subplot(111, projection='3d')

ax.ticklabel_format(axis="z", style="sci", scilimits=(0,0))

# plt.title('Matplot surface plot', size='xx-large', loc='left')
#title properties

surf = ax.plot_trisurf(df['X'], df['Y'], df['Result'], cmap=cm.jet,
linewidth=1)

fig.colorbar(surf, pad=-0.05, shrink=1.0, format='%.1e', orientation=
'vertical',
             drawedges='False', aspect=10)
plt.title('MeV/Cm$^2$', size='x-large', loc='right')
```

```
ax.set_xlabel('cm', labelpad=20, size='x-large') #labelpad to
offset labels
ax.set_ylabel('cm', labelpad=20, size='x-large')
ax.set_zlabel('MeV/cm$^2$', labelpad=20, size='x-large')
fig.tight_layout()
# These hide the z axis for contour. Comment out for surface

# Single view
ax.view_init(elev=35, azim=20) #elev is angle (elev=90, azim=225)
for contour
plt.show()

fig.savefig("Pu_tc_hetero_meshtal_1.pdf", bbox_inches='tight')
```

Appendix C: Excerpts from Preliminary MCNP MMRTG Input

```
c ------------------------------------------- Begin Cell Cards
c
c ------------------------------------------- level 1
c
c - fuel pellets
1 1 -11.68 39 -40 -50 IMP:p=1 $Pellet 1
2 1 -11.68 39 -40 -53 IMP:p=1 $Pellet 2
3 1 -11.68 33 -34 -50 IMP:p=1 $Pellet 3
4 1 -11.68 33 -34 -53 IMP:p=1 $Pellet 4
c
c
c
c - Carbon spacers
5 3 -1.95 36 -37 -51 IMP:p=1
6 3 -1.95 36 -37 -54 IMP:p=1
c
c
c
c - Internal voids
7 0 37 -38 -51 IMP:p=1
8 0 37 -38 -54 IMP:p=1
9 0 35 -36 -51 IMP:p=1
10 0 35 -36 -54 IMP:p=1
c
c
```

```
c
c - Iridium Shells
11 2 -22.56 38 -41 -51 #1 IMP:p=1
12 2 -22.56 38 -41 -54 #2 IMP:p=1
13 2 -22.56 32 -35 -51 #3 IMP:p=1
14 2 -22.56 32 -35 -54 #4 IMP:p=1
c
c
c
c
.............................................
.............................................
c - TC Lattices
c - Lower
208 0  501 -505  402 -403 201 -204 fill=4 IMP:p=1
209 0 -700  604  703 -702 201 -204 fill=8 IMP:p=1
210 0  401 -405  502 -503 201 -204 fill=2 IMP:p=1
211 0  600 -704 -603  602 201 -204 fill=6 IMP:p=1
212 0  504 -500  402 -403 201 -204 fill=4 IMP:p=1
213 0 -603  602  705 -601 201 -204 fill=6 IMP:p=1
214 0  404 -400  502 -503 201 -204 fill=2 IMP:p=1
215 0  703 -702 -605  701 201 -204 fill=8 IMP:p=1
c
c
c
c
.............................................
.............................................
```

```
c - Heat Fins
701 9 -2.84 10 -18 303 -304 901 -902 IMP:p=1
c
702 9 -2.84 10 -18 303 -304 905 -906 IMP:p=1
c
703 9 -2.84 10 -18 303 -304 903 -904 IMP:p=1
c
704 9 -2.84 10 -18 303 -304 -907 908 IMP:p=1
c
.................................................
.................................................
c ------------------------------------------- Physics
c
c
c
sdef erg=D1 pos=4.629  4.7775 0 axs=0 0 1 rad=d2 ext = d3 par=p
c      cel= d4
.................................................
.................................................
si2 H 0 6
sp2 -21 1
si3 H 0 44
sp3 D 0 1
si4 L 1 2 3 4 21 22 23 24 41 42 43 44 61 62 63 64
     81 82 83 84 101 102 103 104 121 122 123 124 141 142 143 144
sp4  0.03125 0.03125 0.03125 0.03125 0.03125 0.03125 0.03125 0.03125
     0.03125 0.03125 0.03125 0.03125 0.03125 0.03125 0.03125 0.03125
     0.03125 0.03125 0.03125 0.03125 0.03125 0.03125 0.03125 0.03125
```

```
     0.03125 0.03125 0.03125 0.03125 0.03125 0.03125 0.03125 0.03125
     $ 1/32 = 0.03125
.................................................
.................................................
c Air 0.001205 g/cc
c
M13  6000.03p  0.000124 $ Carbon (nat)
     7000.04p  0.755268 $ Nitrogen
     8000.04p  0.231781 $ Oxygen
     18000.04p 0.012827 $ Argon
c +F4:N   199
Phys:p e
MODE P
c
c
PRINT 110 $ prints first 50 particles locations, directions, and energies
c ctme 1 $bump up for real runs
c NPS 1000000
c
c
c
FMESH14:p GEOM=xyz   ORIGIN= -30 -30 -20 $flux
             IMESH=40   IINTS=1000
             JMESH=40   JINTS=1
             KMESH=60   KINTS=1000
             OUT=ik
```